THESIS

A NONLINEAR SYNTHETIC UNIT HYDROGRAPH METHOD THAT ACCOUNTS FOR CHANNEL NETWORK TYPE

Submitted by

Kelsey A. Czyzyk

Department of Civil and Environmental Engineering

In partial fulfillment of the requirements

For the Degree of Master of Science

Colorado State University

Fort Collins, Colorado

Spring 2018

Master's Committee:

Advisor: Jeffrey D. Niemann

Jorge Gironás
Michael J. Ronayne

ABSTRACT

A NONLINEAR SYNTHETIC UNIT HYDROGRAPH METHOD THAT ACCOUNTS FOR CHANNEL NETWORK TYPE

Stormflow hydrographs are commonly estimated using synthetic unit hydrograph (UH) methods, particularly for ungauged basins. Current synthetic UHs either consider very limited aspects of basin geometry or require explicit representation of the basin flow paths. None explicitly considers the channel network type (i.e., dendritic, parallel, pinnate, rectangular, and trellis). The goal of this study is to develop and test a nonlinear synthetic UH that explicitly accounts for the network type. The synthetic UH is developed using kinematic wave travel time expressions for hillslope and channel points in the basin. The effects of the network structure are then isolated into two random variables whose distributions are estimated based on the network type. The proposed method is applied to ten basins from each classification and compared to other related methods. The results suggest that considering network type improves the estimated UHs with the largest improvements seen for dendritic, parallel, and pinnate networks.

ACKNOWLEDGEMENTS

I would like to thank Mike Coleman for his technical support and processing of the new DEMs. I would also like to thank North Dakota State University Mountain Plains Consortium for financial support. I also thank Jeffrey Niemann, Jorge Gironás, Michael Ronayne, Almoatasem Abdoulhak, and Sediqa Hassani for their helpful suggestions and collaboration on this project. Jorge Gironás thanks Fondecyt Grant 1161439 for additional support on this topic.

TABLE OF CONTENTS

ABSTRACT ii

ACKNOWLEDGEMENTS iii

1. INTRODUCTION 1

2. MODEL DEVELOPMENT 5

2.1 HILLSLOPE TRAVEL TIME DISTRIBUTION 5

2.2 CHANNEL TRAVEL TIME DISTRIBUTION 8

2.3 TOTAL TRAVEL TIME DISTRIBUTION 11

3. APPLICATION TO BASINS 13

4. RESULTS 15

4.1 EVALUATION OF MODEL ASSUMPTIONS 15

4.2 EVALUATION OF MODEL RESULTS 20

5. CONCLUSIONS 25

6. TABLES 29

7. FIGURES 33

8. REFERENCES 44

1. INTRODUCTION

Many widely-used hydrologic models, such as HEC-HMS (Feldman, 2000) and SWAT (Arnold and Fohrer, 2005), represent spatial variability within a watershed using a semi-distributed approach. Despite their simplicity, semi-distributed models have been shown to exhibit similar performance to fully distributed models (Abu El-Nasr et al., 2005; Haghnegahdar et al., 2015; Reed et al., 2004). In this approach, the basin is divided into sub-basins (or hydrologic response units), and within each sub-basin, excess rainfall (or runoff) is generated with little consideration of spatial variability. The excess rainfall is then commonly transformed into stormflow at the sub-basin outlet using a unit hydrograph (UH) method, where the UH method assumes a linear relationship between the excess rainfall and stormflow.

In many cases (particularly ungauged basins), a synthetic UH is used. Commonly-used synthetic UHs include the SCS (1972), Snyder (1938), and Clark (1945) methods (see Singh et al., 2014 for a recent review of synthetic UHs). These methods estimate the UH based on relatively few physical characteristics of the watershed. For example, the original SCS/NRCS method used a single dimensionless UH for all watersheds (SCS, 1972). The dimensionless UH was then rescaled based on the coordinates of the UH peak, where the coordinates were typically calculated using watershed characteristics such as the area, mainstream length, and average watershed slope. More recently, the method was updated so that the dimensionless UH shape can vary based on a selected peaking factor (NRCS, 2007).

Watersheds exhibit differences beyond those directly considered in traditional synthetic UH methods. In particular, they can exhibit very distinct channel network structures depending on the geomorphic conditions under which the networks developed. These differences have led

to network classifications such as dendritic, parallel, pinnate, rectangular, and trellis (Fig. 1) (Howard, 1967; Mejía and Niemann, 2008; Parvis, 1950; Zernitz, 1932). Dendritic networks are tree-like with channels oriented in many directions and acute angles at confluences. This network type develops when few lithologic or topographic constraints are present (Zernitz, 1932). Parallel networks have major channels that are aligned with each other and develop when the region has a pre-existing slope (Castelltort et al., 2009; Howard, 1967; Phillips and Schumm, 1987; Zernitz, 1932). Pinnate networks tend to be feather-like with a single main channel and many smaller channels joining the main channel at acute angles, but the origin of this network type is unclear (Jung et al., 2011; Parvis, 1950; Phillips and Schumm, 1987; Zernitz, 1932). Rectangular networks have channels with right-angle bends and tributaries that merge at right-angles. They form when the channels exploit orthogonal jointing in the bedrock (Howard, 1967). Trellis networks resemble a garden trellis with numerous short tributaries joining irregular main streams. This network type develops in fold-and-thrust belts like the Appalachian Mountains (Parvis, 1950; Zernitz, 1932). Channel networks are often classified by visual inspection, but quantitative methods have been developed to ensure objectivity. These methods include empirical approaches (Argialas et al., 1988; Hadipriono et al., 1990; Ichoku and Chorowicz, 1994) and an approach based on scaling invariance (Mejía and Niemann, 2008). The network classification has also been shown to affect the time of concentration of a watershed. For example, Jung et al. (2017) showed differences in relationships between time of concentration with bifurcation ratio and maximum hydraulic length of flow path between network types.

Several UH methods have been developed to consider channel network structure, but none have explicitly considered network classifications. The Geomorphic Instantaneous UH

estimates the probability density function (PDF) of travel times using Horton's Ratios, which are derived from the network structure (Gupta et al., 1980; Rodríguez-Iturbe and Valdes, 1979). This approach has also been generalized to allow a nonlinear relationship between excess rainfall and stormflow (Rodríguez-Iturbe et al., 1982) and to consider the effects of hillslope travel times (van der Tak and Bras, 1990). However, Horton's ratios were later shown to be insensitive to wide variations in network structure (Kirchner, 1993). Gupta and Waymire (1983) also proposed a geomorphic instantaneous UH based on stream links instead of Strahler (1957) stream ordering. Other UH methods explicitly represent the watershed's flow paths. For example, the modified Clark method in HEC-HMS allows the user to enter a time-area distribution, which describes the distribution of travel times to the watershed outlet, but that time-area distribution must be determined outside of the modeling framework (Feldman, 2000). It is usually found using a digital elevation model (DEM). Similarly, spatially distributed travel time (SDTT) methods explicitly represent the flow paths in a watershed using a DEM (Du et al., 2009; Lee et al., 2008; Maidment, 1993; Muzik, 1996). Then, they calculate a travel time in each DEM grid cell using its physical properties (Du et al., 2009; Zuazo et al., 2014). The UH is then found from the distribution of travel times from the watershed cells to the outlet. Some SDTT methods also overcome the linearity assumption of UH methods because the travel times vary in time (Du et al., 2009; Lee and Yen, 1997). However, SDTT methods operate on the DEM grid and thus cannot be implemented within semi-distributed (or lumped) models.

The objective of this study is to develop and test a nonlinear synthetic UH method that accounts for the network type. The synthetic UH is developed by adapting a SDTT method. It uses kinematic wave theory to derive flood wave travel time expressions for hillslope and channel cells of a DEM. Then, it estimates the required characteristics for each cell (e.g.,

channel slope and width) using simplifications and empirical relationships that are applied throughout the watershed. This step allows the properties of each cell to be estimated based on watershed-wide model parameters. It also isolates the effects of the flow path network in two random variables (one for the hillslopes and one for the channels). These two random variables are then represented using theoretical distributions, and the parameters of those distributions are estimated for the five network types. The resulting synthetic UH is nonlinear and can be implemented inside a semi-distributed (or lumped) model if the user provides the model parameters and selects one of the five network types.

The outline of the paper is as follows. Section 2 presents the analytical framework that is used to determine the synthetic UHs. Section 3 describes the basins that are used to evaluate the model for each network type. Section 4 evaluates the synthetic UH results by comparing them to the results of a SDTT method (which explicitly represents that actual flow paths for each basin). It also considers whether the network types produce substantial differences in the synthetic UHs. Finally, Section 5 summarizes the key conclusions of the study.

2. MODEL DEVELOPMENT

2.1 HILLSLOPE TRAVEL TIME DISTRIBUTION

The flood wave travel time for a hillslope cell is based on an expression derived by Wong (1995), who applied the kinematic wave approach to a sloping plane where flow enters from upslope and is generated locally by excess rainfall. If this expression is combined with Manning's equation and written for a hillslope cell at location *j*, it becomes:

$$\tau_{h,j} = \left(\frac{n_{h,j} L_j}{\sqrt{S_j}} \right)^{0.6} E_j^{-0.4} \left[\left(\lambda_{flow,j} + 1 \right)^{0.6} - \left(\lambda_{flow,j} \right)^{0.6} \right] \quad (1)$$

where $\tau_{h,j}$ is the travel time for hillslope cell j, $n_{h,j}$ is Manning's roughness coefficient, L_j is the flow length, S_j is the slope, E_j is the excess rainfall rate, and $\lambda_{flow,j}$ is the ratio of the flow entering from upslope to the flow that is produced within the plane.

Gironás et al. (2009) modified this expression for use in a SDTT method. The excess rainfall is allowed to vary in time but is constrained to be homogeneous in space, so it becomes E_i where i is an index for time. It is assumed that the excess rainfall is produced uniformly across the basin's DEM, so variable source areas are not considered (Dunne and Black, 1970). Because the excess rainfall rate varies in time, the travel time varies in time and becomes $\tau_{h,i,j}$. In reality, $\lambda_{flow,j}$ also varies in time, but Gironás et al. (2009) made the approximation that $\lambda_{flow,j} = A_{up,j} / A$, where $A_{up,j}$ is the total area that is upslope of the grid cell and A is the area of the grid cell itself. This approach assumes that the duration of the storm is long enough for the entire upslope area to contribute flow simultaneously to the grid cell. This assumption has been made by others (e.g., Melesse and Graham, 2004; Rodríguez-Iturbe et al., 1982) and was

evaluated in detail by Zuazo et al. (2014), who found it to be a good approximation of full kinematic wave routing on hillslopes. Using these approximations, Eq. (1) becomes:

$$\tau_{h,i,j} = \left(\frac{n_{h,j} L_j}{\sqrt{S_j}} \right)^{0.6} E_i^{-0.4} \left[\left(\frac{A_{up,j}}{A} + 1 \right)^{0.6} - \left(\frac{A_{up,j}}{A} \right)^{0.6} \right] \tag{2}$$

Even though every grid cell has the same area A, the length L_j can vary between grid cells to account for flow paths in the diagonal and cardinal directions of the grid.

An expression can then be written for the total hillslope travel time ($T_{h,i,k}$) for flow that starts at any cell *k* in the basin and moves to the basin outlet:

$$T_{h,i,k} = \sum_{j \in \text{Hillslope}} \left(\frac{n_{h,j} L_j}{\sqrt{S_j}} \right)^{0.6} E_i^{-0.4} \left[\left(\frac{A_{up,j}}{A} + 1 \right)^{0.6} - \left(\frac{A_{up,j}}{A} \right)^{0.6} \right] \tag{3}$$

where the summation includes all the hillslope cells on the path between cell k and the basin outlet. Eq. (3) indicates that the hillslope travel time depends on a variety of local characteristics. To simplify the model, three approximations are implemented. First, variation in the local flow length is neglected by replacing L_j with L, which is an effective flow length for all grid cells. Assuming that flow directions are equally likely to occur in all cardinal and diagonal directions, that effective length is the average of the cardinal and diagonal flow lengths of the grid cells ($L = 0.5\left(1+\sqrt{2}\right)A^{0.5}$). Second, all hillslope cells are assumed to have the same roughness n_h, which is frequently assumed when applying similar models (e.g., Gironás et al., 2009; Robinson and Sivapalan, 1996; Zuazo et al., 2014). Third, it is assumed that all hillslope cells have the same effective slope S_h. In reality, most basins tend to have convex-up hillslopes due to slope-dependent transport processes such as rainsplash, bioturbation, and soil creep (Gilbert, 1909; Roering et al., 2001; Tucker and Bras, 1998). However, planar hillslopes are a

common assumption in many similar models (e.g., Gironás et al., 2009; Robinson and Sivapalan, 1996). Using these approximations, the total hillslope travel time becomes:

$$T_{h,i,k} = E_i^{-0.4} n_h^{0.6} S_h^{-0.3} L^{-0.4} \sum_{j \in \text{Hillslope}} L \left[\left(\frac{A_{up,j}}{A} + 1 \right)^{0.6} - \left(\frac{A_{up,j}}{A} \right)^{0.6} \right] \tag{4}$$

To simplify the notation, the constant basin properties are collected into a single hillslope coefficient $m_h \equiv n_h^{0.6} S_h^{-0.3} L^{-0.4}$. In addition, the summation in Eq. (4) is defined as $A_{sh,k}$ where the subscript k is included because each location where flow starts k has a different path to the outlet and thus a different value for that summation. This summation depends on the accumulation of area along the hillslope flow paths, so it is closely related to the aggregation of the flow network. Substituting these variables into Eq. (4), it becomes:

$$T_{h,i,k} = E_i^{-0.4} m_h A_{sh,k} \tag{5}$$

Eq. (5) describes the hillslope travel time from an arbitrary point k to the outlet. For a given storm event, flow is expected to begin at all locations in the basin. Thus, one can consider $A_{sh,k}$ as the outcome (for location k) of a random variable A_{sh}. The variable A_{sh} probabilistically describes the collection of values of $A_{sh,k}$ that occur across the basin. It is assumed that A_{sh} is described by the four-parameter generalized gamma distribution (Harter, 1967; Stacy and Mihram, 1965). This assumption is evaluated later in this paper. The generalized gamma distribution applies to non-negative variables, which is consistent with A_{sh}, and has been widely used to represent UHs (Singh, 1998). The generalized gamma PDF is written as:

$$f(A_{sh}) = \frac{k_h \left(A_{sh} - \gamma_h \right)^{k_h \alpha_h - 1}}{\beta^{k_h \alpha_h} \Gamma\left(\alpha_h \right)} \exp\left[- \left(\frac{A_{sh} - \gamma_h}{\beta_h} \right)^{k_h} \right] \tag{6}$$

where α_h $(\alpha_h > 0)$ is a shape parameter that is primarily associated with the skewness, and k_h $(k_h > 0)$ is a shape parameter that is primarily associated with the kurtosis. γ_h is the location parameter and the distribution's lower bound, and β_h $(\beta_h > 0)$ is the scale parameter. $\Gamma(\cdot)$ represents the gamma function. It is assumed that the distribution parameters α_h, k_h, γ_h, and β_h can be estimated from the network type and maximum upslope area for any hillslope cell $A_{h\max}$. These assumptions and the nature of any such dependence is examined later.

2.2 CHANNEL TRAVEL TIME DISTRIBUTION

A very similar approach is used to calculate the travel time distribution for the channels. The flood wave travel time in a channel cell is based on an expression derived by Wong (2001), who considered a wide rectangular channel where flow enters from both upstream and locally under the kinematic wave approximation. If the Wong (2001) equation is applied to a channel cell at location j, it can be written:

$$\tau_{c,j} = L_j \left(\frac{n_{c,j}}{\sqrt{S_j}} \right)^{0.6} W_j^{0.4} \left[\frac{Q_{down,j}^{0.6} - Q_{up,j}^{0.6}}{Q_{down,j} - Q_{up,j}} \right] \tag{7}$$

where $\tau_{c,j}$ is the travel time in channel cell j, $n_{c,j}$ is Manning's roughness coefficient for the cell, W_j is the channel width, $Q_{down,j}$ is the flow at the downstream end of the cell, and $Q_{\mathrm{up},j}$ is the flow that is contributed to the cell from upstream. Unlike the hillslope cells, which drain relatively small areas, it is unlikely that the entire upstream area simultaneously contributes flow to a channel cell for storms with realistic durations. Following Iacobellis and Fiorentino (2000), it is assumed that only some fraction r of the upstream area contributes flow simultaneously.

Thus, $Q_{up,j} = rE_i A_{up,j}$ and $Q_{down,j} = rE_i \left(A_{up,j} + A \right)$ if excess rainfall is again assumed to be spatially homogeneous.

An expression can then be written for the total channel travel time from a cell *k* in the basin to the basin outlet $T_{c,i,j}$:

$$T_{c,i,k} = \sum_{j \in \text{Channel}} L_j \left(\frac{n_{c,j}}{\sqrt{S_j}} \right)^{0.6} \left(\frac{W_j}{rE_i} \right)^{0.4} \left[\frac{\left(A_{up,j} + A \right)^{0.6} - A_{up,j}^{0.6}}{A} \right] \tag{8}$$

where the summation includes the channel cells on the path between cell k and the outlet.

Several approximations are implemented to simplify Eq. (8). Local variations in cell flow lengths are again neglected by replacing L_j with L, and all channel cells are assumed to have the same roughness n_c, which is a common approach (e.g., Gironás et al., 2009; Zuazo et al., 2014). In addition, the channel slope is assumed to depend on the contributing area according to a power function $S_j = b(A_{up,j} + A)^{-\theta}$ where b and θ are constants that can vary between basins (Flint, 1974; Hack, 1957; Sklar and Dietrich, 2013; Tarboton et al., 1989; Willgoose et al., 1991). The coefficient b is related to the vertical relief of the basin, while θ describes the concavity of the longitudinal profiles of the channels. The slope-area relationship describes the average slope at a given contributing area, but much variation typically occurs around this average value (Cohen et al., 2008; Niemann et al., 2001; Tarboton et al., 1989). In addition, deviations from a power function can also occur (Ijjasz-Vasquez and Bras, 1995). Such complexities are neglected here. Finally, the channel width is also assumed to depend on the contributing area according to a power function $W_j = d(A_{up,j} + A)^e$ where d and e are constants that can vary between basins. Such dependence has been observed empirically (Hack, 1957; Leopold and Maddock, 1953; Montgomery and Gran, 2001; Wolman, 1955) and has been used

in similar models in the past (Snyder et al., 2003). Using these simplifications in Eq. (8), one obtains:

$$T_{c,i,k} = E_i^{-0.4} n_c^{0.6} r^{-0.4} b^{-0.3} d^{0.4} A^{0.3\theta+0.4e-0.4} \sum_{j \in \text{Channel}} L \left(\frac{A_{up,j}}{A} + 1 \right)^{0.3\theta+0.4e} \left[\left(\frac{A_{up,j}}{A} + 1 \right)^{0.6} - \left(\frac{A_{up,j}}{A} \right)^{0.6} \right] \quad (9)$$

To simplify the notation, the constants in front of the summation are collected into a single channel coefficient $m_c \equiv r^{-0.4} n_c^{0.6} b^{-0.3} d^{0.4} A^{0.3\theta+0.4e-0.4}$, and the summation in Eq. (9) is defined as $A_{sc,k}$. This variable describes how area accumulates along the channel flow path and is expected to depend on the channel network structure. Using these definitions, Eq. (10) can be written:

$$T_{c,i,k} = E_i^{-0.4} m_c A_{sc,k} \quad (10)$$

It is assumed that A_{sc} is described by the Johnson special bounded (SB) distribution. This assumption is evaluated later. This distribution is related to the normal distribution, which is associated with sums (George and Ramachandran, 2011; Kottegoda, 1987), and $A_{sc,k}$ is determined by a summation as shown in Eq. (9). The Johnson SB PDF is written:

$$f(A_{sc}) = \frac{\delta_c \lambda_c}{\sqrt{2\pi}\left(A_{sc} - \xi_c\right)\left(\lambda_c - A_{sc} + \xi_c\right)} \exp\left\{ -\frac{1}{2}\left[\gamma_c + \delta_c \ln\left(\frac{A_{sc} - \xi_c}{\lambda_c - A_{sc} + \xi_c} \right) \right]^2 \right\} \quad (11)$$

where γ_c is a shape parameter that primarily controls the skewness, and δ_c $\left(\delta_c > 0\right)$ is a second shape parameter that primarily controls the kurtosis. ξ_c is the location parameter, and λ_c $\left(\lambda_c > 0\right)$ is the scale parameter. This distribution has lower and upper bounds at ξ_c and $\xi_c + \lambda_c$, respectively. It is assumed that the parameters γ_c, δ_c, ξ_c, and λ_c can be estimated based on the

network type and maximum upstream area for any channel cell $A_{\max}$. The nature of any such dependence is examined later.

2.3 TOTAL TRAVEL TIME DISTRIBUTION

The total travel time from an arbitrary point k to the outlet ($T_{i,k}$) is the sum of the hillslope and channel travel times from that point, so one can write:

$$T_{i,k} = T_{h,i,k} + T_{c,i,k} = E_i^{-0.4}\left(m_h A_{sh,k} + m_c A_{sc,k}\right) \tag{12}$$

If the time-invariant portion of the overall travel time is defined as $X_k \equiv m_h A_{sh,k} + m_c A_{sc,k}$, then the PDF for X can be determined by a convolution assuming that $m_h A_{sh,k}$ and $m_c A_{sc,k}$ are independent. The hillslope scale is typically similar irrespective of the hillslope's position in the basin (Tucker et al., 2001), so the hillslope and channel travel times from a point to the outlet are expected to be independent (Rodríguez-Iturbe and Valdes, 1979). Because an analytical solution for this convolution is not known, the convolution is performed numerically:

$$f_X\left(n\Delta X\right) = \sum_{l=0}^{n} f_{m_h A_{sh,k}}\left(l\Delta X\right) f_{m_c A_{sc,k}}\left(n\Delta X - l\Delta X\right) \tag{13}$$

where n is the number of discrete increments of X used in the numerical evaluation, ΔX is the size of the increment, and l is an index for those increments. Finally, the instantaneous UH (IUH) associated with excess rainfall E_i can be found from the PDF for T_i, which is:

$$f_{T_i}\left(T_i\right) = \frac{1}{E_i^{-0.4}} f_X\left(\frac{T_i}{E_i^{-0.4}}\right) \tag{14}$$

The IUH varies in time because E_i varies in time. UHs and direct runoff hydrographs can then be calculated by a convolution of the excess rainfalls and IUHs as described by Gironás et al. (2009).

In summary, this modeling approach isolates the effect of the drainage network structure into the random variables A_{sh} and A_{sc}. The other basin properties are represented by a series of constants: n_h, S_h, n_c, r, b, d, θ, and e. The method also includes two constants that imply the spatial resolution of the calculations: L and A. These constants transform the PDFs for A_{sh} and A_{sc} into the time-invariant PDF for X. Then, the PDF for X is modified using the time-varying excess rainfall rate E_i to determine the time-varying PDF for T_i, which is the time-varying IUH for the basin.

This method is similar to the time-area methods developed by Zoch (1934) and Clark (1945) because it uses travel times that are determined from the basin shape. Those methods used simplified watershed geometries, but that approach has since been generalized to use real watershed configurations (Kull and Feldman, 1998; Peters and Easton, 1996; Saghafian et al., 2002). The proposed model also differs from those methods because the travel times vary in time, which produces a time-varying IUH. The use of time-varying unit hydrographs has also been explored by others (Du et al., 2009; Lee et al., 2008; Xia et al., 2005). Also, those methods used a linear reservoir to represent the attenuation of the flood wave by storage in the basin (Clark, 1945; Zoch, 1934). The effects of including a linear reservoir in the proposed synthetic UH method will be explored later in this paper.

3. APPLICATION TO BASINS

The synthetic UH method is evaluated by application to ten basins from each of the five classifications. Nearly all the basins were originally processed by Mejía and Niemann (2008). In their collection, however, Buckeye Run, WV (dendritic) and Stony Run, WV (trellis) are sub-basins of other included basins. Furthermore, Hill Creek, UT (parallel) does not strongly exhibit parallel characteristics. Thus, these three basins were replaced with Rockcastle Creek, KY (dendritic), Penns Creek, PA (trellis), and Mancos River Tributary, CO (parallel). The new basins were selected from regions where the networks had been previously classified (Mejía and Niemann, 2008).

The new basins were processed in the manner used by Mejía and Niemann (2008). Specifically, the TauDEM toolbox for ArcGIS was used to fill pits, determine flow directions (according to the D8 algorithm), and calculate upslope/upstream areas and slopes (O'Callaghan and Mark, 1984; Tarboton, 2003; Tarboton et al., 1991). To avoid infinite travel times in the model, any zero slope was replaced by the lesser of the calculated slope resolution and 0.8 times the minimum nonzero slope present in the processed DEM. Cells containing channels were identified using thresholds for contributing area and topographic curvature following Montgomery (2001) and Rinaldo et al. (1995). Montgomery (2001) divided the slope-area plot into five geomorphic zones: hillslopes, valley heads, colluvial channels, bedrock channels, and alluvial channels. They suggested that the initiation points for channels occur in the valley head zone, which was identified with an area threshold for each basin. That threshold also determines $A_{h\max}$. For a cell to include a channel, its cell must also be concave up (Rinaldo et al., 1995). Because the calculation of curvature from a DEM is prone to uncertainty, any cell with a

curvature greater than the negative curvature resolution is considered to be concave up (Taylor, 1997). In the model, any hillslope cell contains only a planar hillslope, while a channel cell includes both a channel (through which the upstream flow is directed) and a hillslope (through which any local or upslope flow must pass before entering the channel network). Thus, all excess rainfall must travel over some distance of hillslope before reaching the outlet.

Basic characteristics for the 50 basins are summarized in Table 1. The pinnate basins tend to be larger than the other types with an average area of 1,014 km^2. The parallel and rectangular basins are the smallest with average areas of 217 and 254 km^2, respectively. The pinnate basins also have the coarsest DEM resolutions with an average of 76.4 m, while the DEM resolutions for the remaining types are on average of 27 m. Similarly, $A_{h\max}$ is largest for the pinnate basins (on average 23,710 m^2) and smallest for the dendritic and parallel basins (on average 4,280 and 5,200 m^2, respectively).

4. RESULTS

4.1 EVALUATION OF MODEL ASSUMPTIONS

We first examine the distributions of A_{sh} and A_{sc} for the basins. In order to calculate A_{sc} for any basin, values must be selected for the width-area exponent *e* and the slope-area exponent θ. *e* was assigned a typical value of 0.5 for all basins based on Montgomery and Gran (2001). θ was calculated from the slope-area plot of each basin. It has averages of 0.43, 0.36, 0.40, 0.34, 0.39, for the dendritic, parallel, pinnate, rectangular, and trellis basins, respectively. Because θ might vary with the network type, A_{sc} for a given basin was calculated using that basin's θ value.

Sixteen theoretical distributions were identified as candidates to describe A_{sh} and A_{sc} based on their general properties (e.g., the existence of a lower bound). The parameters of the distributions were estimated for each basin using the maximum likelihood method (Scholz, 2006). The fit of each distribution was then evaluated using the Kolmogorov-Smirnov (K-S) statistic, which is the maximum deviation between the cumulative distribution function (CDF) determined from the DEMs and the theoretical distribution (D'Agostino and Stephens, 1986; Weber et al., 2006). The K-S statistic is not compared to a critical value in a hypothesis test because the observations of A_{sh} and A_{sc} from the DEMs are not independent due to the nested structure of the drainage networks. Thus, they violate the assumptions required to perform such a test (D'Agostino and Stephens, 1986; Jogesh Babu and Rao, 2004).

The K-S statistics for the top three distributions for A_{sh} and A_{sc} are plotted for all the basins in Fig. 2. The three best-fitting distributions for A_{sh} are the four-parameter generalized

gamma, the log-Pearson type III, and the generalized Pareto distributions (Fig. 2a). On average, the generalized gamma distribution fits the observations of A_{sh} best with an average K-S statistic of 0.043. It also has the lowest average K-S statistics for the pinnate and trellis classifications. The log Pearson type III has the lowest average K-S statistics for the remaining three classifications, but it performs worse for the trellis basins and much worse for the pinnate basins than the generalized gamma distribution. Comparing between classifications, the generalized gamma distribution performs best for the dendritic and parallel types and consistently worse for the pinnate basins. It exhibits varying performance for the rectangular and trellis basins, which might suggest that the hillslope aggregation patterns are heterogeneous within these classifications.

The three best-fitting distributions for A_{sc} are the Johnson SB, beta, and generalized extreme value distributions (Fig. 2b). On average, the Johnson SB distribution fits the observed distributions of A_{sc} best with an average K-S statistic of 0.021. The other two distributions have greater variability in their K-S statistics and almost always perform worse than the Johnson SB distribution. Comparing between classifications, the Johnson SB distribution is most successful for the parallel and pinnate types. It again exhibits the most variability in performance for the rectangular and trellis basins.

The left side of Fig. 3 shows histograms of A_{sh} values for a typical basin in each classification along with the fitted PDFs. The A_{sh} histograms have positive skewness and exhibit only subtle differences among the five basins (note the small humps in the PDFs for some basins). In all cases, the generalized gamma distribution fits well. The right side of Fig. 3 shows the similar results for A_{sc}. The A_{sc} histograms differ substantially between the five basins. For

the dendritic basin, the A_{sc} histogram has negative skewness. However, the skewness is approximately zero for the parallel and trellis basins and positive for the pinnate basin. The Johnson SB distribution has sufficient flexibility to adapt to these different shapes.

We next examine whether the parameters of the generalized gamma distribution for A_{sh} can be estimated from the network classification and the hillslope size $A_{h\max}$. For each classification, Fig. 4 plots the calibrated distribution parameters against $A_{h\max}$. Because $A_{h\max}$ is much larger for the pinnate basins, they are shown in separate graphs on the right side of Fig. 4. The shape parameters k_h and α_h and the location parameter γ_h appear to be independent of $A_{h\max}$ and relatively constant within each classification. However, differences are observed between the classifications. For example, the dendritic basins tend to have lower α_h values and higher k_h values than the other basins. Higher k_h values are associated with the humps that were observed in Figs. 3a and 3c. In contrast, the scale parameter β_h depends on $A_{h\max}$ (Fig 4c and g), and the relationship can be approximated by a power function. A power function ensures that the relationship goes through the origin as expected. The relationships between β_h and $A_{h\max}$ also exhibit differences between the classifications. Most notably the pinnate and trellis basins have much flatter relationships than the other three types. The dependence of the A_{sh} parameters on network type is interesting because the types are based on the channels not the hillslopes. These results suggest a connection between the morphology of the hillslopes and channels, either that the flow paths on the hillslopes depend on the channel network structure into which they flow or that the hillslope and fluvial processes that determine the hillslope and channel flow paths are somehow correlated.

We next consider whether the parameters of the Johnson SB distribution for A_{sc} can be estimated from the network type and the basin size $A_{\max}$. For each classification, Fig. 5 plots the calibrated distribution parameters against $A_{\max}$. The shape parameters γ_c and δ_c and location parameter ξ_c do not vary with $A_{\max}$, but differences are observed between the classifications. The most notable differences are observed for γ_c (Fig. 5a), which controls the skewness of the A_{sc} distribution. Dendritic basins have negative γ_c values, while pinnate basins have positive γ_c values (which corresponds to the differences seen for the typical basins in Fig. 3h and Fig. 3f). The skewness also relates to the typical basin shape for each classification (Fig. 1). For example, dendritic basins have an abundance of channel cells far from the basin outlet, which leads to an abundance of large A_{sc} values and negative skewness. Unlike the other distribution parameters, the scale parameter λ_c varies with $A_{\max}$, and this relationship can be approximated with a power function. The relationship also exhibits differences between classifications. Specifically, dendritic, parallel, and rectangular basins have flatter curves than the other two types.

Table 2a provides the average values of k_h, α_h, and γ_h for each classification (and average values for all basins combined). It also provides the fitted power function that estimates β_h from $A_{h\max}$ for each classification (and a fitted power function for all basins combined). Table 2b provides equivalent information for γ_c, δ_c, ξ_c, and λ_c. To determine whether the distribution parameters differ significantly between the network types, an analysis of variance (ANOVA) was employed for the parameters that are independent of $A_{h\max}$ and $A_{\max}$. Specifically, a one-way ANOVA method was used for unadjusted pairwise comparisons between

classifications (Cohen and Cohen, 2008) with a 90% confidence interval (p-value = 0.1). Similarly, an analysis of covariance (ANCOVA) was used to determine whether the coefficients and exponents of the power functions are significantly different between classifications (Maxwell and Delaney, 2004). This analysis was performed by first taking the logarithms of the variables involved and examining whether the intercepts and slopes of the resulting linear relationships are different.

The results of the ANOVA and ANCOVA tests are summarized in Table 3. If a parameter is listed in Table 3, there is a 90% chance that the pair of classifications have different mean values for that parameter. For A_{sh}, 9 out of 10 classification pairings have at least one parameter that is significantly different (Table 3a). For A_{sc}, 8 out of 10 classification pairings have at least one parameter that is significantly different (Table 3b). Most commonly, that parameter is γ_c, which is associated with skewness. Fewer parameters are significantly different for A_{sc} than A_{sh} because the parameters for A_{sc} tend to be more variable within classifications. Overall, these results suggest that the distributions for A_{sh} and A_{sc} are different for the five network types.

To evaluate the reliability of estimating the distribution parameters from the network type (as well as $A_{h\max}$ and $A_{\max}$), the K-S statistic is used once more. Fig. 6 compares the K-S statistics for the basins when the distribution parameters are estimated from three different methods. In Method 1, they are calibrated directly from the A_{sh} and A_{sc} distributions for each basin (i.e. using values shown in Figs. 4 and 5). In Method 2, they are estimated from the classification (using the results for each classification in Table 2). In Method 3, they are estimated without consideration of the classification (using the results for all basins combined in

Table 2). For A_{sh}, 41 of the 50 basins have improved accuracy (lower K-S statistics) when the network type is included (comparing Methods 2 and 3). This improvement occurs across all network types (at least 7 of 10 basins exhibit improvement for each network type). For most classifications, the results of Method 2 are very similar to those of Method 1. In such cases, knowledge of the classification is sufficient to capture the distribution of A_{sh} in an individual basin. For the trellis basins, however, the K-S statistics for Method 2 remain more similar to those of Method 3, which suggests that information about each basin is more valuable for estimating the distribution of A_{sh}.

For A_{sc} 34 of the 50 basins have improved accuracy (lower K-S statistics) when the network type is included (comparing Methods 2 and 3). This improvement is greatest for dendritic, parallel, and pinnate network types, while rectangular and trellis networks show little improvement. Rectangular and trellis networks can have a wide variety of basin shapes and thus a variety of A_{sc} distributions. The variability within those classifications makes it more difficult to estimate the A_{sc} distributions from the classification alone. Overall, estimating the parameters from the network type is more successful for A_{sh} than A_{sc} because the distributions for A_{sh} are less variable within each classification.

4.2 EVALUATION OF MODEL RESULTS

The synthetic UH method is tested by comparing the IUHs for four cases. Case 1 explicitly considers the individual cell slopes and the actual flow paths for each basin. This method is equivalent to a SDTT method and is considered the correct IUH. Case 2 replaces the individual cell slopes with the estimates from S_h and the slope-area relationship, and it replaces

the actual A_{sh} and A_{sc} distributions with the calibrated theoretical distributions. This case evaluates the assumptions that are required to construct a synthetic UH method. Case 3 estimates the parameters of the theoretical distributions based on the network classification. This is the classification-based synthetic UH method. Case 4 estimates the parameters of the theoretical distributions irrespective of the network classification. This case is analogous to current synthetic UH methods.

For this comparison, most of the parameters were set to constant values for all 50 basins to reduce confounding effects (Table 4). The selected Manning's roughness for the hillslopes n_h corresponds to short-grass prairie (McCuen et al., 2002). The roughness for channels n_c corresponds to a low-slope stream with weeds and stones or a mountain stream with cobbles and boulders (Chow, 1959). The fraction of area contributing flow r falls within the range for humid to arid climates (0.2 to 0.5) (Iacobellis and Fiorentino, 2000). The width-area coefficient d is a typical value (Montgomery and Gran, 2001). The *b* value varies between basins and is estimated from each basin's slope-area plot (as determined from each basin's DEM). For Cases 2 through 4, the average hillslope slope from the DEM of each basin was used for S_h. The average values for S_h are 0.21 m/m, 0.26 m/m, 0.08 m/m, 0.19 m/m, and 0.21 m/m for dendritic, parallel, pinnate, rectangular, and trellis network types, respectively.

Fig. 7 compares the IUHs from all four cases for a typical basin in each classification (the same basins considered in Figs. 1 and 3). The observed IUHs (Case 1) exhibit notable differences between the classifications. The IUH for the dendritic basin is negatively skewed, the IUH for the pinnate basin is positively skewed, and the IUHs for the other basins are nearly symmetrical. These tendencies are similar to those observed for the A_{sc} distributions for the

same basins (Fig. 3) and all the basins (Fig. 4). For the dendritic basin, when the slopes are approximated and the theoretical distribution is used (Case 2), the IUH shifts to the right but maintains a similar shape. This shift occurs because the travel times depend nonlinearly on slope. Thus, using average slope for a given contributing area is not equivalent to using the distribution of slopes for that contributing area. The proposed synthetic UH method (Case 3) closely approximates the previous two cases. This similarity suggests that considering the classification alone provides an adequate approximation of the individual basin's IUH. The case that neglects the classification (Case 4) has nearly zero skew and is a poor match for the observed IUH (Case 1). The other basins exhibit similar results. Cases 2 and 3 remain close to the observed IUH, and Case 4 is usually the poorest approximation.

Four metrics are used to quantify the difference in performance between the proposed method (Case 3) and the case that neglects classification (Case 4) for all 50 basins (Fig. 8). The first metric is the Root Mean Squared Error (RMSE) (Moriasi et al., 2007; Singh et al., 2005) where Case 1 is considered the observed IUH (Fig 8a). The second metric is the Nash-Sutcliffe Coefficient of Efficiency (NSCE) (Nash and Sutcliffe, 1970). Because larger NSCE values indicate better performance (in contrast with the other metrics), Fig 8b instead shows 1 – NSCE so that lower values indicate better performance. The third metric is the absolute error in IUH peak value (Fig. 8c), and the fourth metric is the absolute error in the time of the IUH peak (Fig. 8d). In Fig. 8, the columns show the average performance for each classification, and black bars show the range of performance within each classification.

By all four measures, considering network classification greatly improves the average performance and reduces the range in performance for parallel and pinnate basins. For these two classifications, considering the network type produces errors that are about half the errors when

network type is neglected. Parallel basins' average RMSE values considering classification are 56% lower than average RMSE values when type is neglected. In addition, the range of RMSE values when considering network type is 34% lower than when network type is neglected. When considering network type for pinnate basins, the average RMSE and range of RMSE values are 47% and 66% lower than neglecting network type respectively. Considering network classification also improves the performance for dendritic basins for three out of the four measures (all but the error in the IUH peak value). However, the improvements for dendritic basins are smaller than those for parallel and pinnate basins. The average RMSE when considering network type is 21% lower than neglecting network type for dendritic basins. Only small improvements in performance are observed for rectangular and trellis basins, which suggests that basin-specific knowledge is needed to accurately estimate the IUHs for those classifications (again due to the diversity of basin shapes that occur within those classifications). The average RMSE for rectangular and trellis network types when considering classification is lower than neglecting classification by 2% and 4%, respectively.

The IUHs presented so far have been derived based on the distribution of travel times, but storage delays might also be important. To examine whether the differences between classifications persist when storage effects are included, a linear reservoir is added to the calculation of the IUHs. In this case, the total time to the outlet is the sum of the travel time plus the storage delay. Thus, the IUH can be generated by a convolution of the travel time distribution with the storage delay distribution. For a linear reservoir, the storage delay G has an exponential distribution (Chow et al., 1988), which can be written as:

$$f(G) = \frac{e^{-G/K}}{K} \tag{15}$$

where K is the reservoir time constant. For this analysis, the reservoir time constant is assumed to be 60% of the time of concentration (McCuen et al., 2002).

The IUHs with storage delays are shown in Fig. 9 for the example basins. The IUHs are now all positively skewed (a similar effect was observed by Rinaldo et al., 1995). The differences between the classifications are smaller than those in Fig. 7 but still evident (particularly in the width and height of the IUH peak). Furthermore, considering the classification still provides better estimates of the IUHs than neglecting it. Fig. 10 shows the four performance metrics for all 50 basins when the storage delays are included in the IUH. The same general tendencies are observed with and without the storage delays (Figs. 8 and 10). However, the improvement of performance that is achieved by considering network classification is somewhat reduced when storage delays are included (note the differences in the vertical axes between Figs. 8 and 10).

The RMSE in the IUHs from the synthetic method was also calculated when the assumed parameter values were varied from those shown in Table 4 (Fig. 11). Overall, the RMSE decreases when the hillslope roughness n_h increases, the channel roughness n_c increases, the width-area coefficient d increases, the slope-area coefficient b decreases, the fraction of area contributing flow r decreases, the excess rainfall E_i decreases, and the linear reservoir constant K increases. It remains almost unchanged as the average hillslope slope S_h changes.

5. CONCLUSIONS

This study developed and tested a nonlinear synthetic UH method that explicitly accounts for the network type (dendritic, parallel, pinnate, rectangular, and trellis). Within this approach, the network structure was isolated in two random variables A_{sh} and A_{sc}, which characterize the flow paths for the hillslopes and channels, respectively. Based on this analysis, the following conclusions can be made:

1. Among the sixteen theoretical distributions tested, the four-parameter gamma distribution best describes the observed distributions of A_{sh} and the Johnson SB distribution best describes the observed distributions of A_{sc}. For A_{sh}, the shape and location parameters of the gamma distribution are independent of the hillslope size $A_{h\max}$, but the scale parameter depends on $A_{h\max}$. Similarly, for A_{sc}, the shape and location parameters of the Johnson SB distribution are independent of the basin size $A_{\max}$, but the scale parameter depends on $A_{\max}$.
2. The distributions of A_{sh} are significantly different between the five network classifications. Based on ANOVA and ANCOVA results, 9 out of 10 classification pairings have at least one distribution parameter that is significantly different. Because the classifications are determined from the channel network structure, this result suggests that the flow paths on the hillslopes (which determine A_{sh}) depend on the type of channel network into which they flow.
3. The distributions of A_{sc} are significantly different between the five classifications. From the ANOVA and ANCOVA results, 8 out of 10 classification pairings have at least one

distribution parameter that is significantly different. The parameter that usually differs between classification pairs controls the skewness of the A_{sc} distribution. Dendritic basins have an abundance of locations that are distant from the outlet, which produces an abundance of large A_{sc} values and a negative skewness. In contrast, pinnate basins have more locations that are close to the outlet, which produces many small A_{sc} values and positive skewness. The other network types tend to have more symmetrical distributions for A_{sc}.

4. The A_{sh} distributions are more accurately estimated based on the network type than the A_{sc} distributions. The A_{sh} distributions exhibit relatively small differences between classifications but are relatively consistent within classifications, which allows accurate estimation of the distribution parameters. For A_{sc}, the differences within classifications are greater. Overall, the network type is more useful for estimating the A_{sc} distribution for dendritic, parallel, and pinnate networks, than for rectangular and trellis networks.
5. The IUHs from a SDTT method without storage delays typically differ between the five network classifications. Much like the A_{sc} distributions, the IUHs of dendritic basins are negatively skewed, the IUHs for pinnate basins are positively skewed, and the IUHs for the other classifications are approximately symmetrical. When storage delays are included, the differences between classifications are smaller but remain present. These differences suggest that the network type can impact the hydrologic response of a watershed.
6. The proposed synthetic UH method, which estimates the A_{sh} and A_{sc} distributions based on the network classification, provides better estimates of the SDTT IUHs than a method

that neglects classification. The improved performance occurs both when storage effects are neglected and included. The greatest improvements in performance are observed for the parallel and pinnate classifications. Moderate improvements are also observed for dendritic basins, while only small improvements are observed for rectangular and trellis basins. Basins within the parallel and pinnate classifications tend to have very similar basin shapes and flow path structures, which makes it easier to estimate their IUHs based only on the classification. Basins within the rectangular and trellis classifications tend to be more diverse, so it is more important to explicitly represent an individual basin's flow paths.

Overall, the results show that the five network classifications have differences in their IUHs and that considering network classification provides improved estimates of the IUHs. The classification-based synthetic UH has the potential to be used in semi-distributed models, but more testing is required. Independent validation should be performed by applying the method to basins that are not used in the model development. Testing on smaller basins is also needed. The results generated in this study considered large basins, but semi-distributed models often consider much smaller sub-basins. Most distribution parameters in the model are independent of basin size and the dependence on basin size was included for the remaining distribution parameters, so the method is expected to apply to smaller basins. However, it should be tested to understand the implications on the method's performance. Further analyses of the interaction of channel network type and hillslope flow paths should also be performed. In particular, how does the role of the channel network type change as the active hillslope processes change? In addition, the assumption that a constant fraction of upstream area contributes flow at each time should be further analyzed. For example, a relationship between this fraction and basin size or

grid cell location in the basin could be considered. The assumption that excess rainfall is produced uniformly across the basin could also be changed. In particular, the differences in behavior between channel network types may differ if variable source areas produce the excess rainfall. Also, the IUHs from the proposed method were evaluated by comparing to those from a SDTT model that explicitly represents the slopes and flow paths with the basin. Future research should evaluate the performance when the method is used to reproduce observed hydrographs. Such comparisons would allow testing of other assumptions in the method (e.g., the use of kinematic wave theory).

6. TABLES

Table 1. Basic characteristics of the 50 basins that are analyzed in this study.

	Basin Name	Outlet Lat. (deg)	Outlet Long. (deg)	DEM Resolution (m)	Basin Area (km^2)	Channel Threshold (m^2)
DENDRITIC	Bluestone Creek, WV	39.3020	-80.7787	27.2	324	4,400
	Buffalo Creek, WV	40.2509	-80.5976	27.0	419	5,100
	Captina Creek, OH	39.8706	-80.8193	27.0	460	3,600
	Cedar Creek, GA	31.6712	-81.5048	28.5	219	4,900
	Little Saluda River, SC	34.0773	-81.5942	28.1	565	4,700
	Rockcastle Creek, KY	38.0020	-82.5189	27.9	314	3,100
	Tenmile Creek, PA	39.9804	-80.0240	27.0	512	4,400
	Turkey Creek, SC	33.7773	-82.1606	30.0	625	4,500
	Tygarts Creek, KY	38.3926	-82.9601	27.4	291	3,700
	Wheeling Creek, WV	40.0506	-80.6673	27.0	739	4,400
PARALLEL	Albert Creek, WY	41.5065	-110.6095	26.8	439	6,500
	Black Sulphur Creek, CO	39.8676	-108.2931	27.1	266	4,400
	Duck Creek, CO	39.9787	-108.3820	27.0	142	5,100
	Greasewood Creek, CO	40.1301	-108.4126	27.0	61	4,400
	Mancos River Trib., CO	37.0950	-108.5070	28.3	113	5,300
	Piceance Tributary 1, CO	39.8884	-108.3959	27.1	156	3,700
	Piceance Tributary 2, CO	39.8620	-108.2998	27.1	74	5,100
	Sheep Creek, WY	41.5645	-110.6154	26.8	487	5,000
	Willow Creek, UT	39.4223	-109.6293	27.2	350	4,400
	Yellow Creek, CO	39.9654	-108.3898	27.1	85	8,100
PINNATE	Dniester Tributary 1, UKR	47.9145	30.6362	75.9	2,114	23,100
	Dniester Tributary 2, UKR	48.1245	30.0062	75.8	1,356	17,200
	Dniester Tributary 3, UKR	46.3545	28.9412	76.8	1,005	23,600
	Dniester Tributary 4, UKR	46.7937	29.9804	76.4	1,573	29,200
	Dniester Tributary 5, UKR	46.6145	29.2845	76.7	967	21,000
	Dniester Tributary 6, UKR	47.1395	28.9062	76.4	761	23,400
	Nistru Tributary 1, MDA	47.3795	30.5062	76.2	697	29,100
	Nistru Tributary 2, MDA	47.3895	30.5562	76.4	589	23,300
	Nistru Tributary 4, MDA	46.1112	28.6129	76.8	723	23,600
	Nistru Tributary 5, MDA	46.0529	28.7587	76.8	350	23,600
RECTANGULAR	Boquet River, NY	44.2423	-73.4620	26.2	241	8,200
	Boreas River, NY	43.8320	-74.0709	26.3	218	5,500
	Cold River NY	44.1037	-74.3126	26.2	218	8,200
	Hudson River, NY	43.9681	-74.0526	26.3	198	9,000
	Saint Regis River, NY	44.5320	-74.4723	26.1	344	4,800
	Salmon River, NY	44.8673	-74.2970	26.1	495	6,800
	Schroon River, NY	43.9556	-73.7337	26.3	239	8,300
	Summer Brook, NY	44.4076	-74.0837	26.1	147	6,100
	Walker Brook, NY	44.0004	-73.7126	26.2	133	10,300
	W. Br. St. Regis River, NY	44.4387	-74.5912	26.1	304	5,500
TRELLIS	Aughwick Creek, PA	40.2987	-77.8873	27.0	823	7,300
	Cacapon River, WV	39.2533	-78.4549	28.0	865	5,500
	Chestuee Creek, TN	35.2451	-84.6565	27.9	339	3,900
	Evitts Creek, MD	39.6640	-78.7320	27.1	240	6,600
	Jackson River, VA	39.1651	-79.7509	27.4	251	4,500
	Juniata River, PA	40.5070	-77.4381	27.5	539	7,800
	Middle Creek, PA	40.7643	-76.8845	26.8	219	8,600
	Penns Creek, PA	40.85756	-77.4606	27.5	480	8,300
	Peters Run, WV	38.7229	-79.3043	27.3	609	7,500
	Sleepy Creek, WV	39.6206	-78.1459	27.1	294	10,300

Table 2. Estimated parameters for (a) the generalized gamma distribution for A_{sh} and (b) the Johnson SB distribution for A_{sc}.

(a) Generalized Gamma Distribution Parameters for A_{sh}

	α_h	k_h	γ_h	β_h
Dendritic	0.296	3.08	0.103	$4.91\, A_{h\max}^{0.265}$
Parallel	0.395	2.35	0.147	$5.07\, A_{h\max}^{0.261}$
Pinnate	0.318	2.86	0.474	$20.5\, A_{h\max}^{0.195}$
Rectangular	0.410	2.15	0.117	$2.72\, A_{h\max}^{0.313}$
Trellis	0.443	2.10	0.102	$34.1\, A_{h\max}^{0.081}$
All	0.372	2.51	0.188	$0.142\, A_{h\max}^{0.588}$

(b) Johnson SB Distribution Parameters for A_{sc}

	γ_c	δ_c	ξ_c	λ_c
Dendritic	-0.544	1.002	-1477	$3760\, A_{\max}^{0.222}$
Parallel	-0.274	0.988	-476	$1163\, A_{\max}^{0.376}$
Pinnate	0.332	0.961	-323	$1428\, A_{\max}^{0.437}$
Rectangular	-0.022	0.988	-307	$450\, A_{\max}^{0.568}$
Trellis	-0.080	0.899	-378	$659\, A_{\max}^{0.520}$
All	-0.118	1.36	-592	$398\, A_{\max}^{0.601}$

Table 3. Distribution parameters that exhibit significant differences between the network classifications based on the analysis of variance (ANOVA) and analysis of covariance (ANCOVA) tests. For the scale parameters β_h and λ_c, β_{h-coef} and λ_{c-coef} refer to the coefficients and $\beta_{h-\exp}$ $\lambda_{c-\exp}$ refer to the exponents in the power functions.

(a) Generalized Gamma Distribution Parameters for A_{sh}

	DEN	PAR	PIN	REC	TRE
DEN		k_h, α_h, γ_h	γ_h	k_h, α_h	k_h, α_h
PAR			k_h, α_h, γ_h	–	α_h, γ_h $\beta_{h-coef}, \beta_{h-\exp}$
PIN				k_h, α_h, γ_h	α_h, γ_h $\beta_{h-coef}, \beta_{h-\exp}$
REC					$\beta_{h-coef}, \beta_{h-\exp}$

(b) Johnson SB Distribution Parameters for A_{sc}

	DEN	PAR	PIN	REC	TRE
DEN		γ_c, ξ_c	γ_c, ξ_c	γ_c, ξ_c	γ_c, ξ_c
PAR			γ_c	γ_c	–
PIN				γ_c	γ_c
REC					–

Table 4. Model parameters used in the development of the instantaneous unit hydrographs. Parameters that vary are determined from the digital elevation model for each basin.

Parameter	Value	Units
Channel roughness (n_c)	0.05	$s/m^{1/3}$
Hillslope roughness (n_h)	0.15	$s/m^{1/3}$
Grid cell area (A)	Varies	m^2
Grid cell length (L)	Varies	m
Slope of hillslopes (S_h)	Varies	m/m
Vertical relief slope factor (b)	Varies	$m^{-2\theta}$
Vertical relief slope exponent (θ)	Varies	-
Width factor (d)	0.02	m^{1-2e}
Width exponent (e)	0.5	-
Fraction of area contributing (r)	0.3	m^2/m^2
Excess rainfall (E_i)	25.4	mm/hr
Linear Reservoir Storage Coefficient	60	%
Step (ΔX)	0.1	m

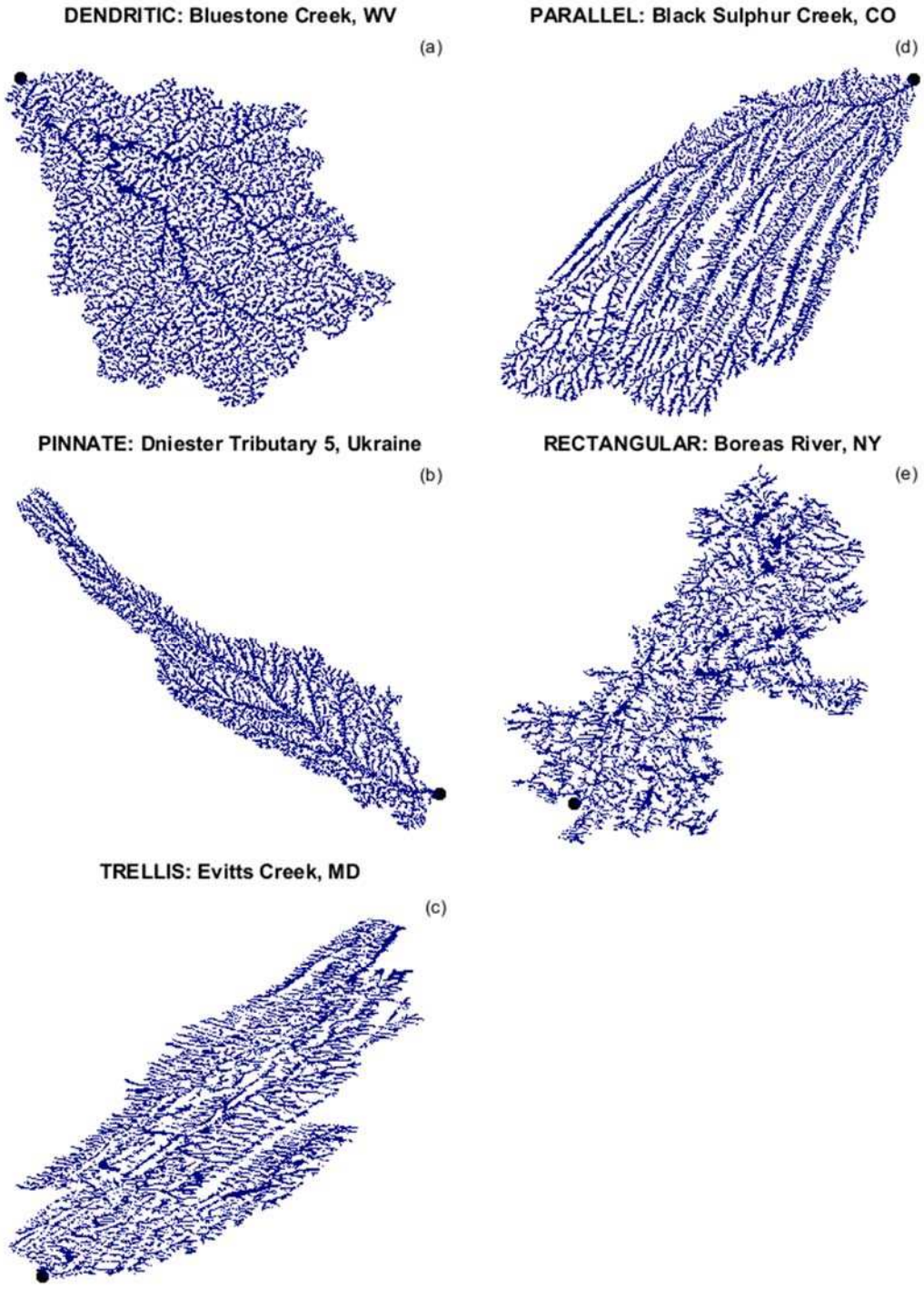

Figure 1. A typical channel network from each network classification. Black dots indicate the basin outlets.

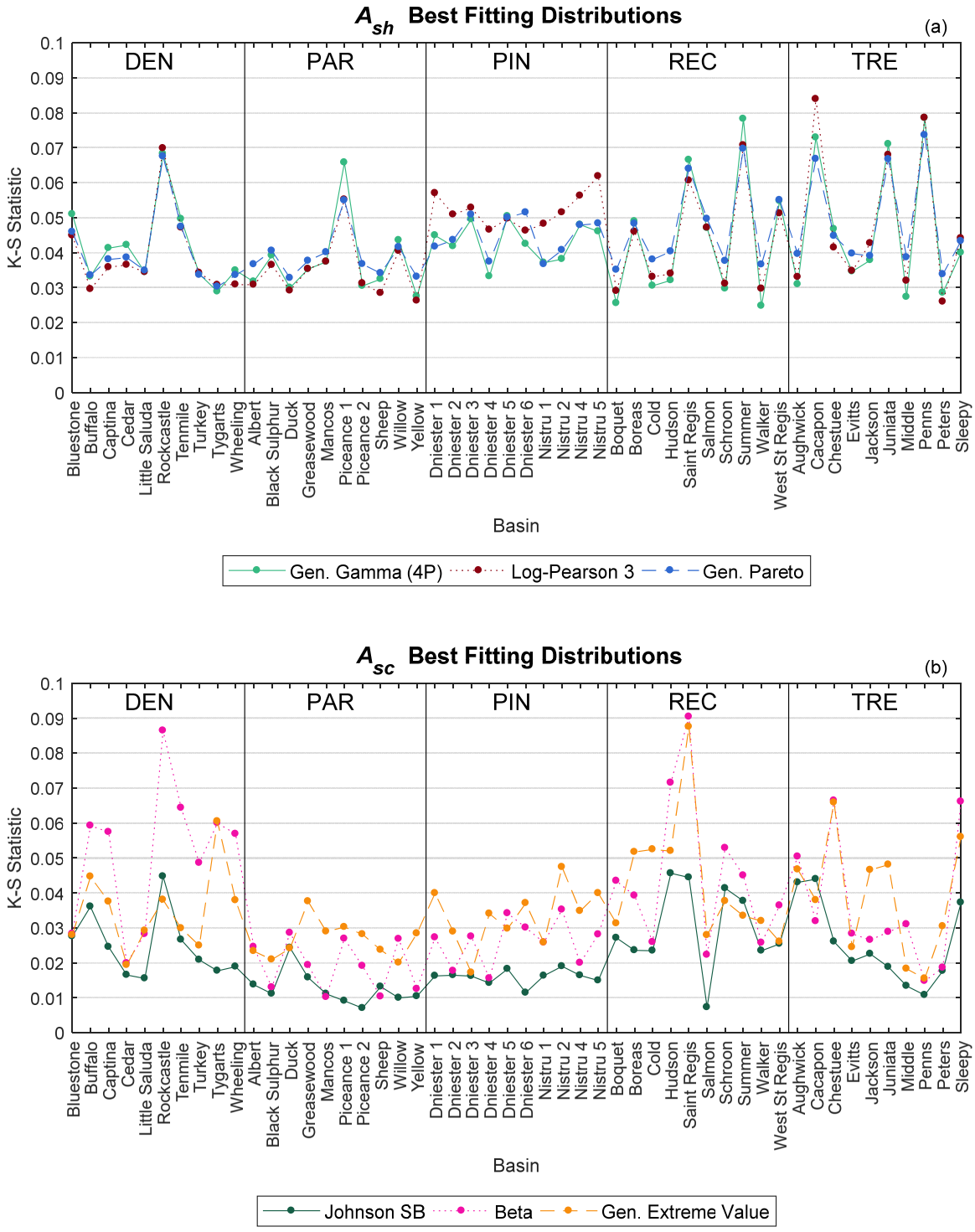

Figure 2. Kolmogorov-Smirnov (K-S) statistics for the three best fitting distributions for (a) A_{sh} and (b) A_{sc}.

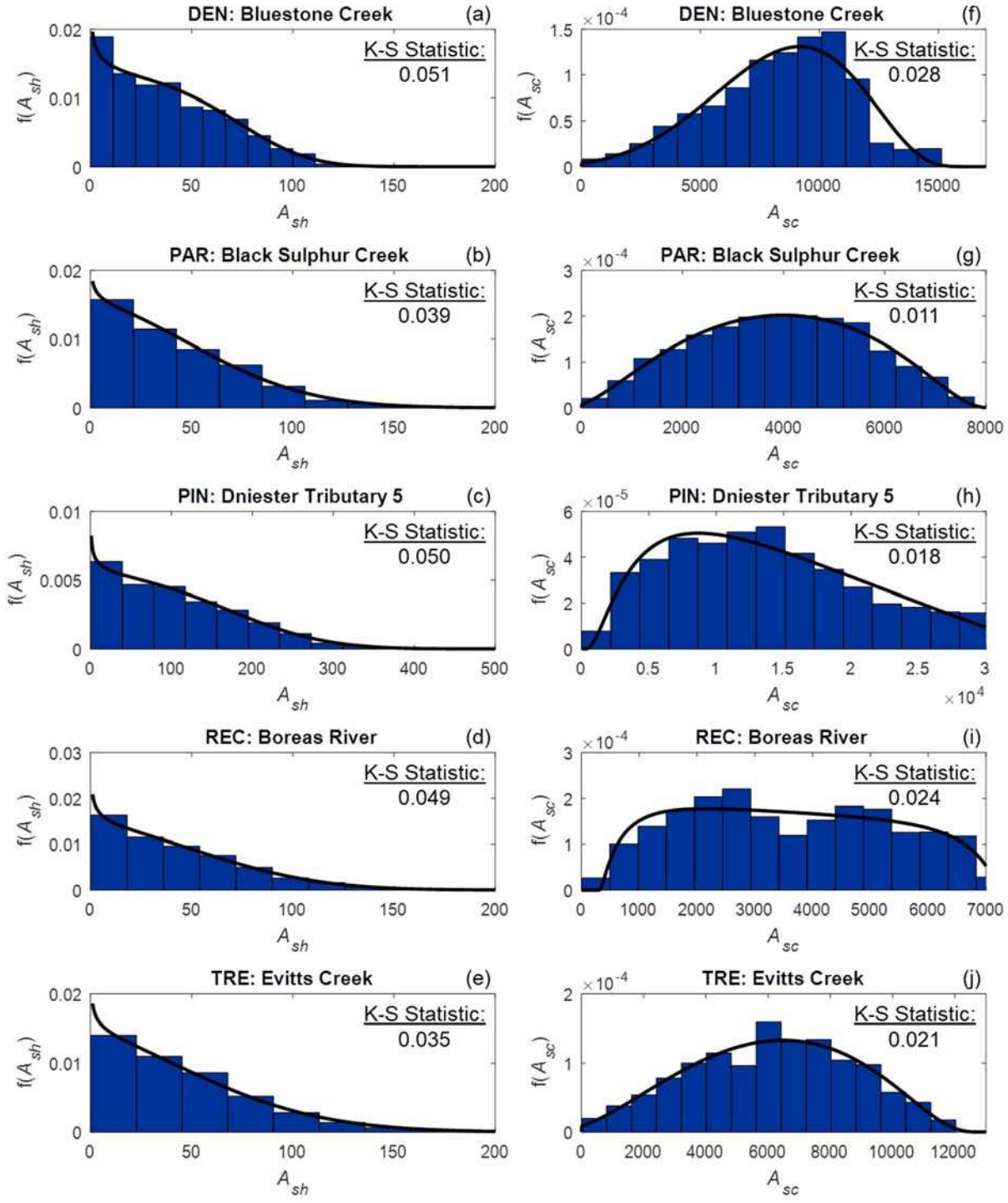

Figure 3. (a) – (e) Histograms and fitted generalized gamma distributions for A_{sh} for a typical basin in each classification, and (f) – (j) histograms and fitted Johnson SB distributions for A_{sc} for the same basin in each classification. Basins are the same as those shown in Fig. 1.

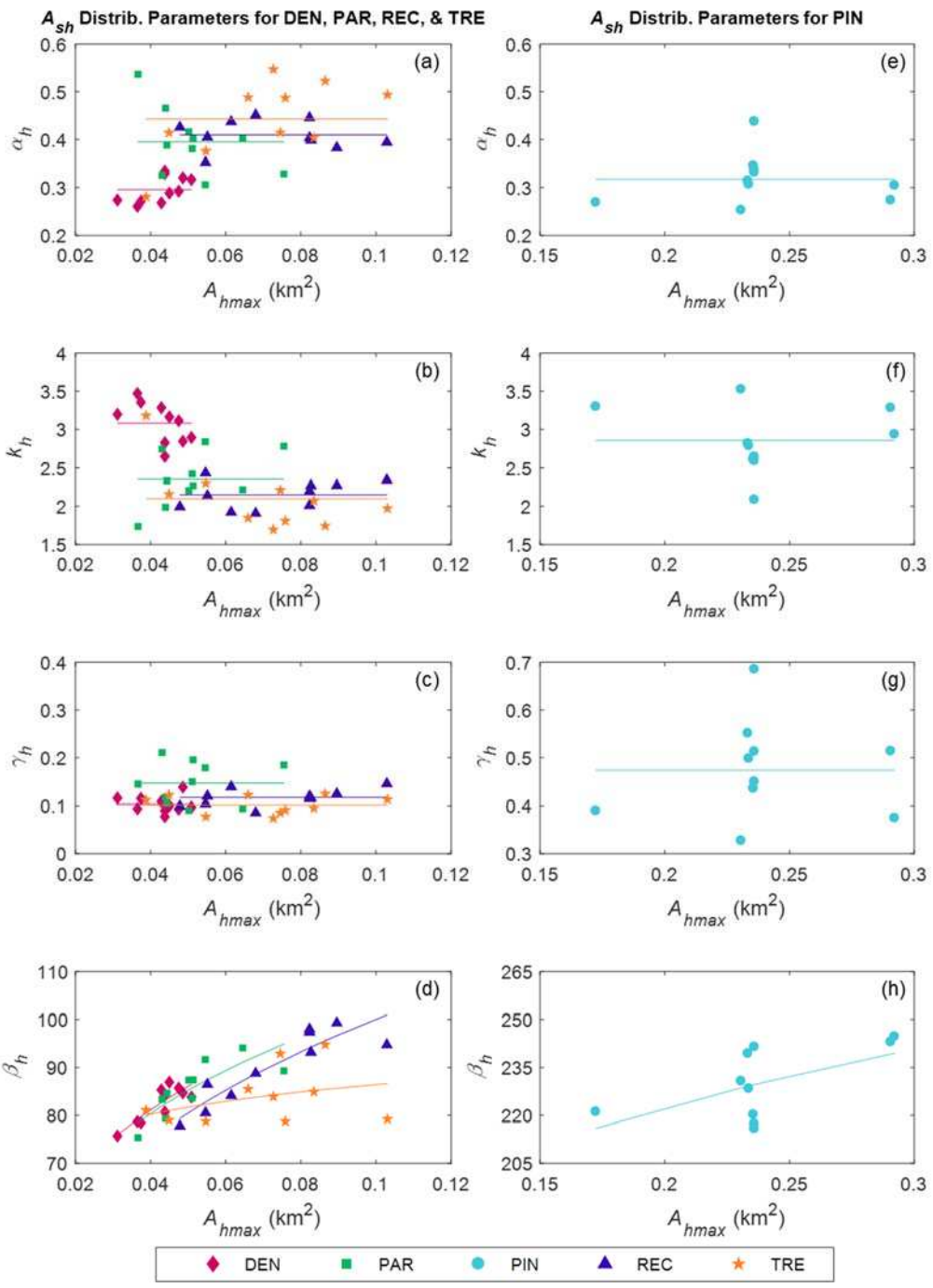

Figure 4. (a) – (d) Parameters of the generalized gamma distribution for A_{sh} for the dendritic, parallel, rectangular, and trellis classifications plotted against the maximum hillslope area A_{hmax} and (e) – (f) parameters of the generalized gamma distribution for A_{sh} for the pinnate classification plotted against A_{hmax}. The individual points represent the calibrated parameter values for each of the 50 basins. The horizontal lines are the average parameter values for each network type in (a) – (c) and (e) – (g). Calibrated β_h values are fitted with a power function in (d) and (h).

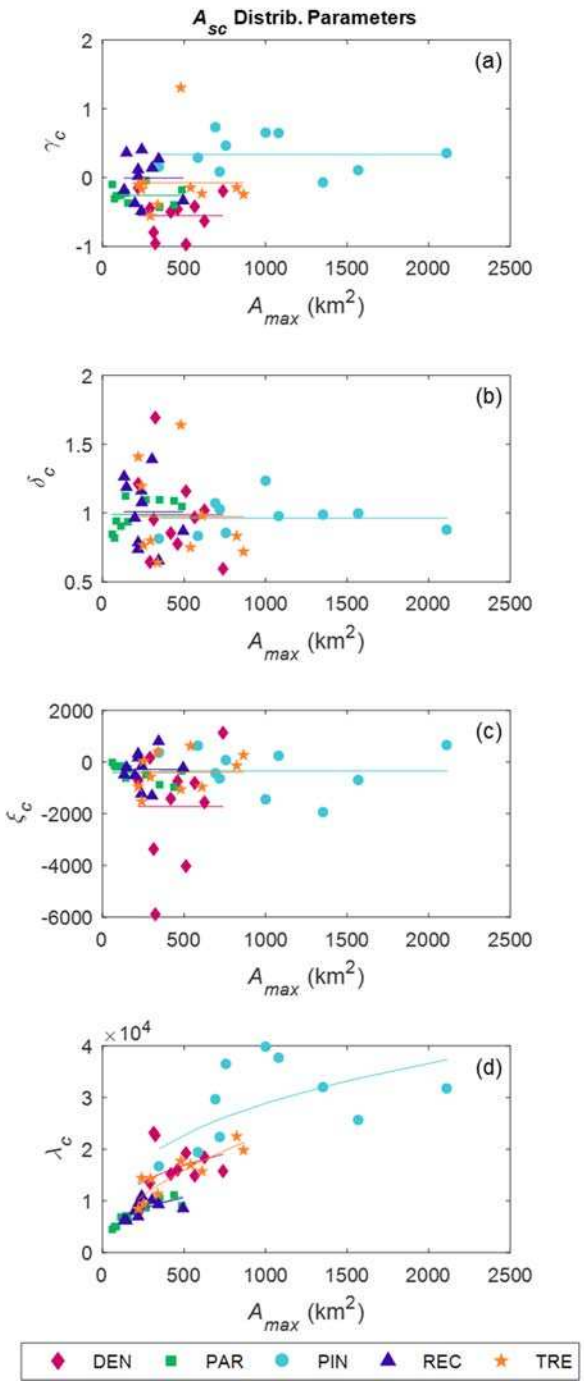

Figure 5. Parameters of the Johnson SB distribution for A_{sc} for all five network classifications plotted against the maximum upstream area A_{max}. The individual points represent the calibrated parameter values for each of the 50 basins. The horizontal lines are the average parameter values for each network type in (a) – (c). Calibrated λ_c values are fitted with a power function in (d).

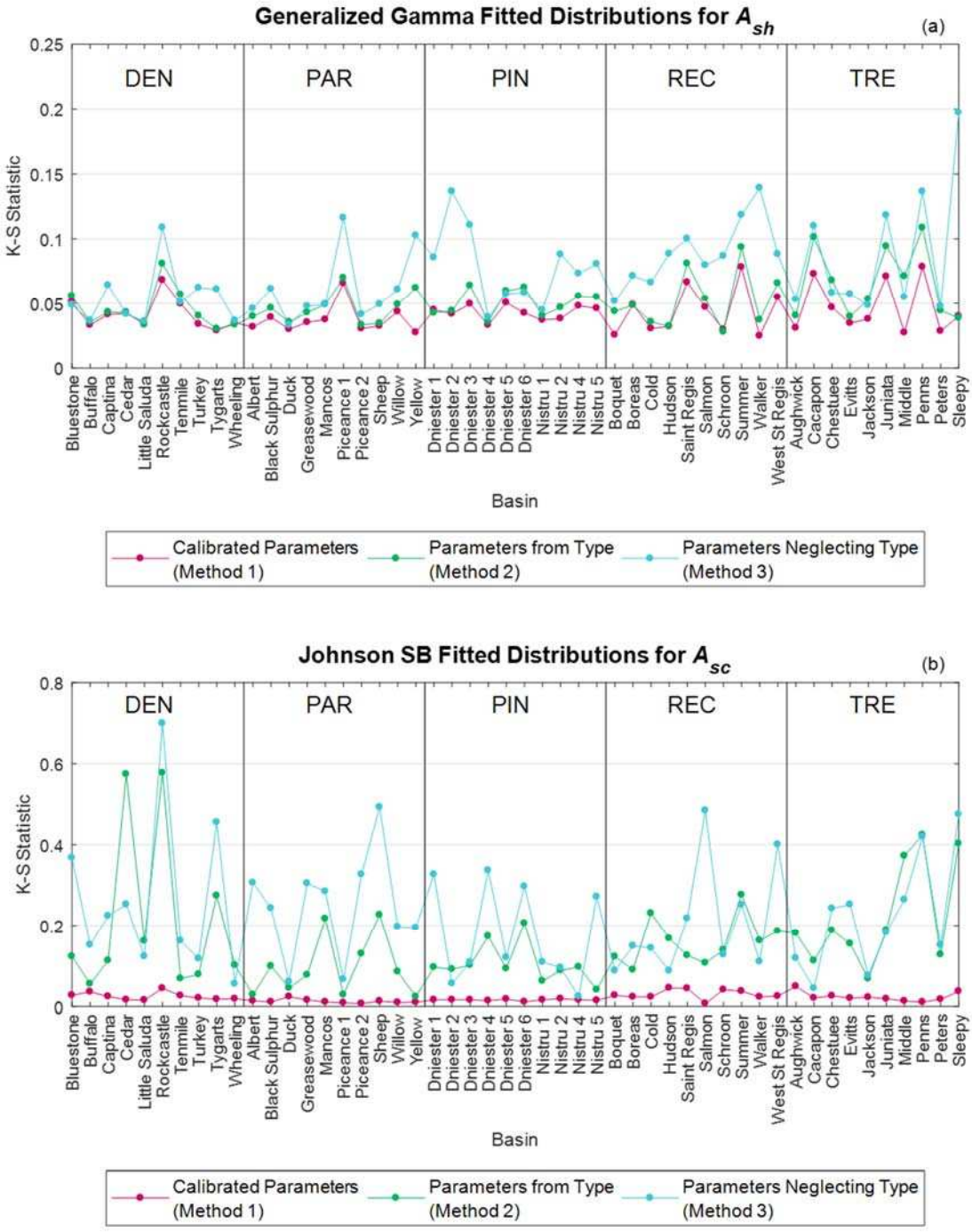

Figure 6. Kolmogorov-Smirnov (K-S) statistics for (a) the generalized gamma distribution for A_{sh} and (b) the Johnson SB distribution for A_{sc} when the distribution parameters are estimated separately for each network (Method 1), based on the network classification (Method 2), and neglecting the network classification (Method 3).

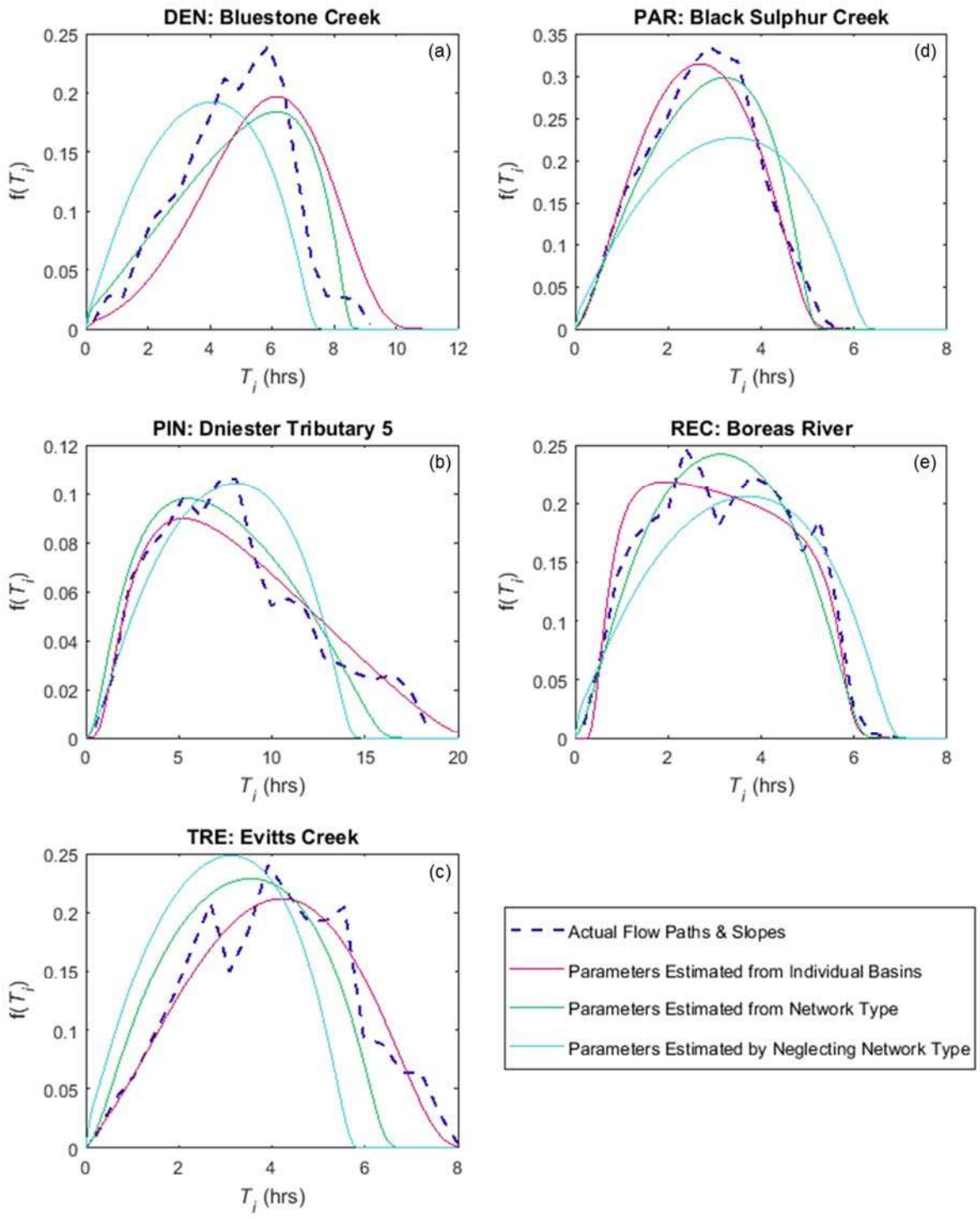

Figure 7. Instantaneous unit hydrographs (IUHs) for a typical basin in each network classification when the IUH is determined for the four cases described in the legend. Basins are the same as shown in Fig. 1.

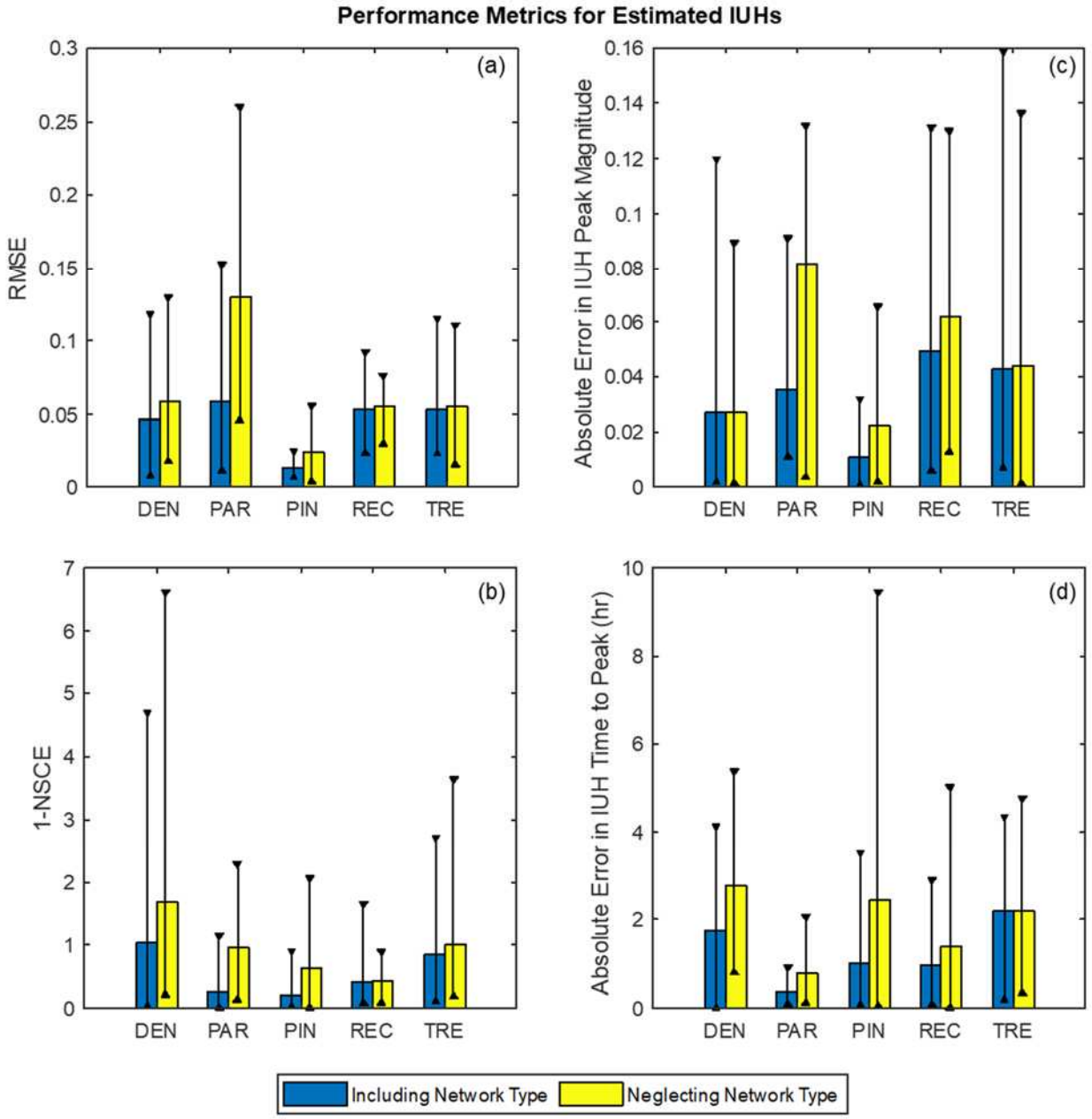

Figure 8. Performance metrics when the instantaneous unit hydrographs (IUHs) are estimated by either including or neglecting the network classification. Column heights indicate the average performance and black bars indicate the range of performance for each case.

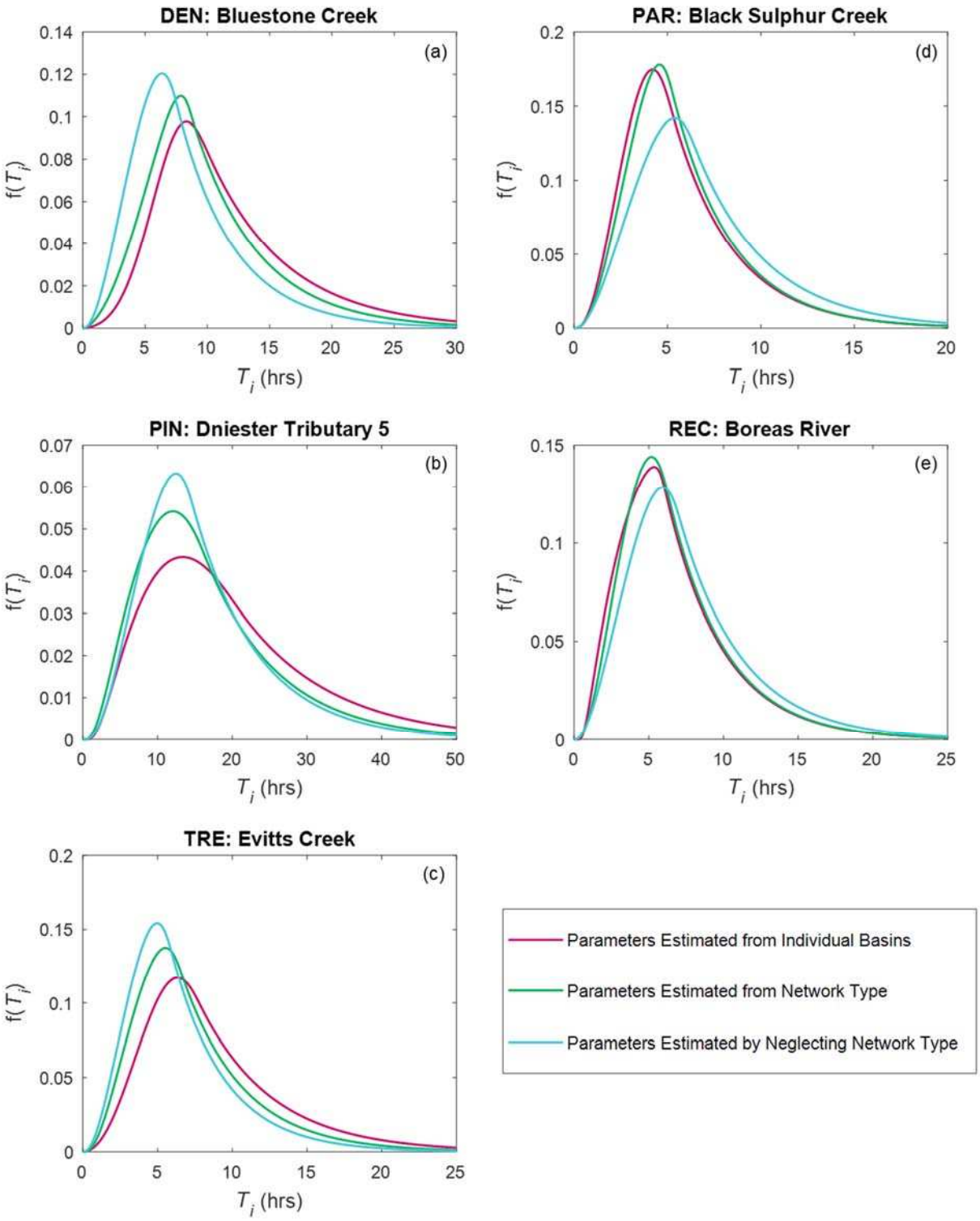

Figure 9. Instantaneous unit hydrographs (IUHs) for a typical basin in each classification when a linear reservoir is included in the determination of the IUH.

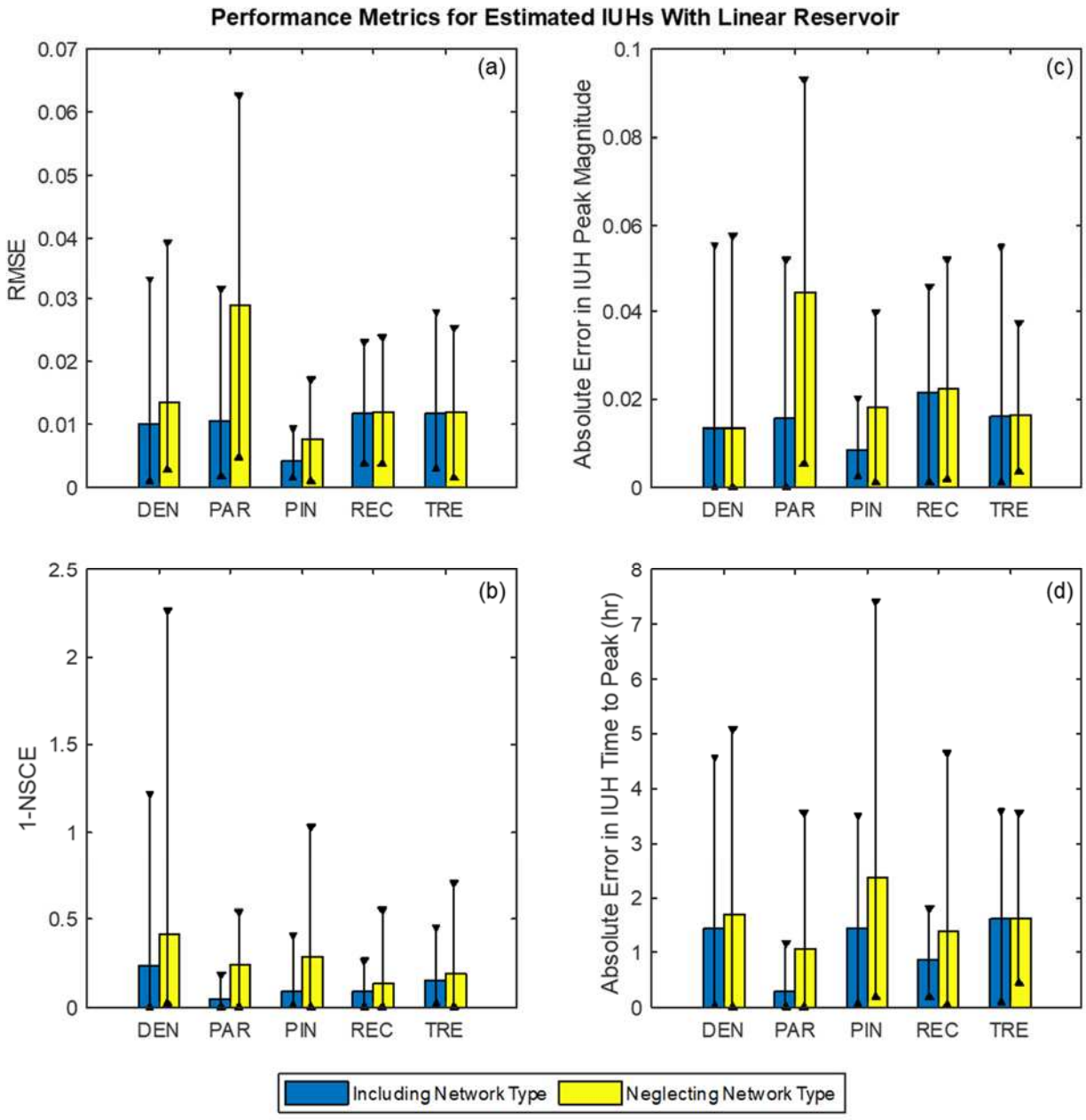

Figure 10. Performance metrics when the instantaneous unit hydrographs (IUHs) are estimated by either including or neglecting network type and a linear reservoir is included. Column heights indicate the average performance and black bars indicate the range of performance for each case.

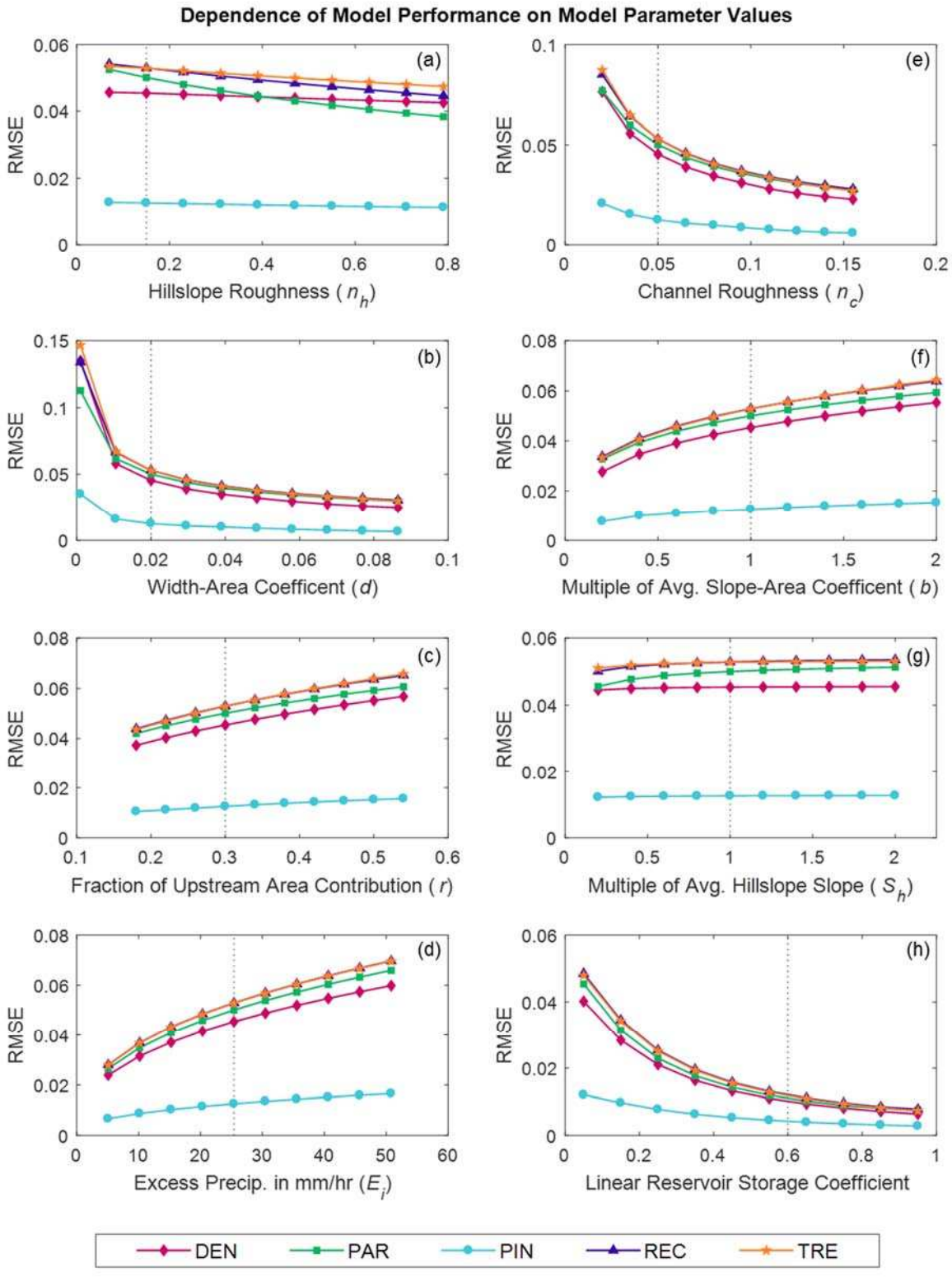

Figure 11. The root mean squared error (RMSE) of the instantaneous unit hydrographs (IUHs) determined from network types as the assumed values of model parameters change. Dashed vertical lines indicate the values used in preceding analyses.

8. REFERENCES

Abu El-Nasr, A., Arnold, J.G., Feyen, J., Berlamont, J., 2005. Modelling the hydrology of a catchment using a distributed and a semi-distributed model. Hydrol. Process. 19, 573–587. doi:10.1002/hyp.5610

Argialas, D., Lyon, J., Mintzer, O., 1988. Quantitative description and classification of drainage patterns. Photogramm. Eng. Remote Sensing 54, 505–509.

Arnold, J.G., Fohrer, N., 2005. SWAT2000: Current capabilities and research opportunities in applied watershed modelling. Hydrol. Process. 19, 563–572. doi:10.1002/hyp.5611

Castelltort, S., Simpson, G., Darrioulat, A., 2009. Slope-control on the aspect ratio of river basins. Terra Nov. 21, 265–270. doi:10.1111/j.1365-3121.2009.00880.x

Chow, V.T., 1959. Open-channel Hydraulics, McGraw-Hil. ed. McGraw-Hill, New York.

Chow, V.T., Maidment, D.R., Mays, L.W., 1988. Unit Hydrograph, in: Applied Hydrology. McGraw-Hill Series in Water Resources and Environmental Engineering, pp. 201–233.

Clark, C.O., 1945. Storage and the Unit Hydrograph. Proc. Am. Soc. Civ. Eng 69, 1333–1360.

Cohen, S., Willgoose, G., Hancock, G., 2008. A methodology for calculating the spatial distribution of the area-slope equation and the hypsometric integral within a catchment. J. Geophys. Res. Earth Surf. 113. doi:10.1029/2007JF000820

Cohen, Y., Cohen, J.Y., 2008. Analysis of Variance, in: Statistics and Data with R. John Wiley & Sons, Ltd, Chichester, UK, pp. 463–509. doi:10.1002/9780470721896.ch15

D'Agostino, R.B., Stephens, M.A. (Eds.), 1986. Goodness-of-Fit Techniques. Marcel Dekker, Inc., New York, NY. doi:10.2307/1165059

Du, J., Xie, H., Hu, Y., Xu, Y., Xu, C.Y., 2009. Development and testing of a new storm runoff

routing approach based on time variant spatially distributed travel time method. J. Hydrol. 369, 44–54. doi:10.1016/j.jhydrol.2009.02.033

Dunne, T., Black, R.D., 1970. Partial Area Contributions to Storm Runoff in a Small New England Watershed. Water Resour. Res. 6, 1296–1311. doi:10.1029/WR006i005p01296

Feldman, A.D., 2000. Hydrologic modeling system HEC-HMS, U.S. Army Corps of Engineers Technical Reference Manual. doi:CDP-74B

Flint, J.J., 1974. Stream gradient as a function of order, magnitude, and discharge. Water Resour. Res. 10, 969–973. doi:10.1029/WR010i005p00969

George, F., Ramachandran, K.M., 2011. Estimation of Parameters of Johnson's System of Distributions. J. Mod. Appl. Stat. Methods 10, 494–504. doi:10.22237/jmasm/1320120480

Gilbert, G.K., 1909. The Convexity of Hilltops. J. Geol. 17, 344–350. doi:10.1086/621620

Gironás, J., Niemann, J.D., Roesner, L.A., Rodriguez, F., Andrieu, H., 2009. A morpho-climatic instantaneous unit hydrograph model for urban catchments based on the kinematic wave approximation. J. Hydrol. 377, 317–334. doi:10.1016/j.jhydrol.2009.08.030

Gupta, V.K., Waymire, E., 1983. On the formulation of an analytical approach to hydrologic response and similarity at the basin scale. J. Hydrol. 65, 95–123. doi:10.1016/0022-1694(83)90212-3

Gupta, V.K., Waymire, E., Wang, C.T., 1980. A representation of an instantaneous unit hydrograph from geomorphology. Water Resour. Res. 16, 855–862. doi:10.1029/WR016i005p00855

Hack, J.T., 1957. Studies of longitudinal stream profiles in Virginia and Maryland, Geological Survey Professional Paper 294-B.

Hadipriono, F.C., Lyon, J.G., Li, T., 1990. The development of a knowledge based expert system

for analysis of drainage patterns. Photogramm. Eng. Remote Sens. 56, 905–909.

Haghnegahdar, A., Tolson, B.A., Craig, J.R., Paya, K.T., 2015. Assessing the performance of a semi-distributed hydrological model under various watershed discretization schemes. Hydrol. Process. 29, 4018–4031. doi:10.1002/hyp.10550

Harter, H.L., 1967. Maximum-Likelihood Estimation of the Parameters of a Four-Parameter Generalized Gamma Population from Complete and Censored Samples. Technometrics 9, 159–165. doi:10.1080/00401706.1967.10490449

Howard, A.D., 1967. Drainage Analysis in Geologic Interpretation: A Summation. Am. Assoc. Pet. Geol. Bull. 51, 2246–2259. doi:10.1306/5D25C26D-16C1-11D7-8645000102C1865D

Iacobellis, V., Fiorentino, M., 2000. Derived distribution of floods based on the concept of partial area coverage with a climatic appeal. Water Resour. Res. 36, 469–482. doi:0042-1397/00/1999WR900287

Ichoku, C., Chorowicz, J., 1994. A numerical approach to the analysis and classification of channel network patterns types : Water Resour. Res. 30, 161–174.

Ijjasz-Vasquez, E.J., Bras, R.L., 1995. Scaling regimes of local slope versus contributing area in digital elevation models. Geomorphology 12, 299–311. doi:10.1016/0169-555X(95)00012-T

Jogesh Babu, G., Rao, C.R., 2004. Goodness-of-fit tests when parameters are estimated. Indian J. Stat. 66, 63–74.

Jung, K., Marpu, P.R., Ouarda, T.B.M.J., 2017. Impact of river network type on the time of concentration. Arab. J. Geosci. 10, 546. doi:10.1007/s12517-017-3323-3

Jung, K., Niemann, J.D., Huang, X., 2011. Under what conditions do parallel river networks occur? Geomorphology 132, 260–271. doi:10.1016/j.geomorph.2011.05.014

Kirchner, J.W., 1993. Statistical inevitability of Horton's laws and the apparent randomness of stream channel networks. Geology 21, 591–594. doi:10.1130/0091-7613(1993)021<0591:SIOHSL>2.3.CO;2

Kottegoda, N.T., 1987. Fitting Johnson SB Curve by the Method of Maximum Likelihood to Annual Maximum Daily Rainfalls. Water Resour. Res. 23, 728–732.

Kull, D.W., Feldman, A.D., 1998. Evolution of Clark's Unit Graph Method to Spatially Distributed Runoff. J. Hydrol. Eng. 3, 9–19. doi:10.1061/(ASCE)1084-0699(1998)3:1(9)

Lee, K.T., Chen, N.-C., Chung, Y.-R., 2008. Derivation of variable IUH corresponding to time-varying rainfall intensity during storms. Hydrol. Sci. J. 53, 323–337. doi:10.1623/hysj.53.2.323

Lee, K.T., Yen, B.C., 1997. Geomorphology and Kinematic-Wave–Based Hydrograph Derivation. J. Hydraul. Eng. 123, 73–80. doi:10.1061/(Asce)0733-9429(1997)123:1(73)

Leopold, L.B., Maddock, T.J., 1953. The Hydraulic Geometry of Stream Channels and Some Physiographic Implications, Geological Survey Professional Paper 252. doi:10.1016/S0169-555X(96)00028-1

Maidment, D.R., 1993. GIS and hydrological modeling, Environmental Modeling within GIS. Oxford: University Press, New York, NY.

Maxwell, S., Delaney, H., 2004. Designing experiments and analyzing data: A model comparison perspective, Briefings in functional genomics proteomics. Taylor & Fancis Group, LLC., New York, NY. doi:10.1002/sim.4780100917

McCuen, R.H., Johnson, P.A., Ragan, R.M., 2002. Highway Hydrology: Hydraulic Design Series No. 2. Arlington, VA.

Mejía, A.I., Niemann, J.D., 2008. Identification and characterization of dendritic, parallel,

pinnate, rectangular, and trellis networks based on deviations from planform self-similarity. J. Geophys. Res. 113, F02015. doi:10.1029/2007JF000781

Melesse, A.M., Graham, W.D., 2004. Storm Runoff Prediction Based on a Spatially Distributed Travel Time Method Utilizing Remote Sensing and GIS. J. Am. Water Resour. Assoc. 9007, 863–879.

Montgomery, D.R., 2001. Slope distributions, threshold hillslopes, and steady-state topography. Am. J. Sci. 301, 432–454. doi:10.2475/ajs.301.4-5.432

Montgomery, D.R., Gran, K.B., 2001. Downstream variations in the width of bedrock channels. Water Resour. Res. 37, 1841–1846.

Moriasi, D.N., Arnold, J.G., Van Liew, M.W., Bingner, R.L., Harmel, R.D., Veith, T.L., 2007. Model Evaluation Guidelines for Systematic Quantification of Accuracy in Watershed Simulations. Trans. ASABE 50, 885–900. doi:10.13031/2013.23153

Muzik, I., 1996. Flood modelling with GIS-derived distributed unit hydrographs. Hydrol. Process. 10, 1401–1409. doi:10.1002/(SICI)1099-1085(199610)10:10<1401::AID-HYP469>3.0.CO;2-3

Nash, J.E., Sutcliffe, J. V., 1970. River flow forecasting through conceptual models part I - A discussion of principles. J. Hydrol. 10, 282–290. doi:10.1016/0022-1694(70)90255-6

Niemann, J.D., Bras, R.L., Veneziano, D., Rinaldo, A., 2001. Impacts of surface elevation on the growth and scaling properties of simulated river networks. Geomorphology 40, 37–55. doi:10.1016/S0169-555X(01)00036-8

NRCS, 2007. Hydrographs, in: National Engineering Handbook. U.S. Departmetn of Agriculture, Washington, D.C., p. 16.

O'Callaghan, J.F., Mark, D.M., 1984. The extraction of drainage networks from digital elevation

data. Comput. Vision, Graph. Image Process. 28, 323–344. doi:10.1016/S0734-189X(84)80011-0

Parvis, M., 1950. Drainage pattern significance in airphoto identification of soils and bedrocks. Photogramm. Eng. 16, 375–409.

Peters, J.C., Easton, D.J., 1996. Runoff Simulation Using Radar Rainfall Data. J. Am. Water Resour. Assoc. 32, 753–760. doi:10.1111/j.1752-1688.1996.tb03472.x

Phillips, L.F., Schumm, S.A., 1987. Effect of regional slope on drainage networks. Geology. doi:10.1130/0091-7613(1987)15<813:EORSOD>2.0.CO

Reed, S., Koren, V., Smith, M., Zhang, Z., Moreda, F., Seo, D.J., 2004. Overall distributed model intercomparison project results, in: Journal of Hydrology. pp. 27–60. doi:10.1016/j.jhydrol.2004.03.031

Rinaldo, A., Vogel, G.K., Rigon, R., Rodriguez-Iturbe, I., 1995. Can One Gauge the Shape of a Basin? Water Resour. Res. 31, 1119–1127. doi:10.1029/94WR03290

Robinson, J.J.S., Sivapalan, M., 1996. Instantaneous Response Functions of Overland Flow and Subsurface Stormflow for Catchment Models. Hydrol. Process. 10, 845–862. doi:10.1002/(SICI)1099-1085(199606)10:6<845::AID-HYP375>3.0.CO;2-7

Rodríguez-Iturbe, I., Valdes, J.B., 1979. The Geomorpholic Structure of Hydrologic Response. Water Resour. Res. 15, 1409–1420. doi:10.1029/WR015i006p01409

Rodríguez-Iturbe, I., González-Sanabria, M., Bras, R.L., 1982. A geomorphoclimatic theory of the instantaneous unit hydrograph. Water Resour. Res. 18, 877–886. doi:10.1029/WR018i004p00877

Roering, J.J., Kirchner, J.W., Dietrich, W.E., 2001. Hillslope evolution by nonlinear, slope-dependent transport: Steady state morphology and equilibrium adjustment timescales. J.

Geophys. Res. 106, 26787. doi:10.1029/2001JB900018

Saghafian, B., Julien, P.Y., Rajaie, H., 2002. Runoff hydrograph simulation based on time variable isochrone technique. J. Hydrol. 261, 193–203. doi:10.1016/S0022-1694(02)00007-0

Scholz, F.W., 2006. Maximum Likelihood Estimation, in: Encyclopedia of Statistical Sciences. John Wiley & Sons, Inc., Hoboken, NJ, USA. doi:10.1002/0471667196.ess1571.pub2

SCS, 1972. SCS National Engineering Handbook. Section 4, Hydrology, in: National Engineering Handbook.

Singh, J., Knapp, H.V., Arnold, J.G., Demissie, M., 2005. Hydrological modeling of the Iroquois River watershed using HSPF and SWAT. JAWRA J. Am. Water Resour. Assoc. 41, 343–360. doi:10.1111/j.1752-1688.2005.tb03740.x

Singh, P.K., Mishra, S.K., Jain, M.K., 2014. A review of the synthetic unit hydrograph: from the empirical UH to advanced geomorphological methods. Hydrol. Sci. J. 59, 239–261. doi:10.1080/02626667.2013.870664

Singh, V.P., 1998. Gamma Distribution, in: Entropy-Based Parameter Estimation in Hydrology. Springer, Dordrecht, pp. 202–203. doi:10.1007/978-94-017-1431-0

Sklar, L., Dietrich, W.E., 2013. River Longitudinal Profiles and Bedrock Incision Models: Stream Power and the Influence of Sediment Supply, in: Rivers Over Rock: Fluvial Processes in Bedrock Channels. American Geophysical Union, p. 237. doi:10.1029/GM107p0237

Snyder, F.F., 1938. Synthetic unit-graphs. Trans. Am. Geophys. Union 19, 447–454. doi:10.1029/TR019i001p00447

Snyder, N.P., Whipple, K.X., Tucker, G.E., Merritts, D.J., 2003. Importance of a stochastic

distribution of floods and erosion thresholds in the bedrock river incision problem. J. Geophys. Res. 108. doi:10.1029/2001JB001655

Stacy, E.W., Mihram, G.A., 1965. Parameter Estimation for a Generalized Gamma Distribution. Technometrics 7, 349–358. doi:10.1080/00401706.1965.10490268

Strahler, A.N., 1957. Quantitative analysis of watershed geomorphology. Eos, Trans. Am. Geophys. Union 38, 913–920. doi:10.1029/TR038i006p00913

Tarboton, D.G., 2003. Terrain Analysis Using Digital Elevation Models (TauDEM, ver. 5.3.5), in: 23rd ESRI International Users Conference.

Tarboton, D.G., Bras, R.L., Rodriguez-Iturbe, I., 1991. On the extraction of channel networks from digital elevation data. Hydrol. Process. 5, 81–100. doi:10.1002/hyp.3360050107

Tarboton, D.G., Bras, R.L., Rodriguez-Iturbe, I., 1989. Scaling and elevation in river networks. Water Resour. Res. 25, 2037–2051. doi:10.1029/WR025i009p02037

Taylor, J., 1997. Introduction to Error Analysis, the Study of Uncertainties in Physical Measurements, 2nd Edition, University Science Books. Sausalito, CA.

Tucker, G.E., Bras, R.L., 1998. Hillslope processes, drainage density, and landscape morphology. Water Resour. Res. 34, 2751–2764. doi:10.1029/98WR01474

Tucker, G.E., Catani, F., Rinaldo, A., Bras, R.L., 2001. Statistical analysis of drainage density from digital terrain data. Geomorphology 36, 187–202. doi:10.1016/S0169-555X(00)00056-8

van der Tak, L.D., Bras, R.L., 1990. Incorporating hillslope effects into the geomorphologic instantaneous unit hydrograph. Water Resour. Res. 26, 2393–2400. doi:10.1029/WR026i010p02393

Weber, M.D., Leemis, L.M., Kincaid, R.K., 2006. Minimum Kolmogorov-Smirnov test statistic

parameter estimates. J. Stat. Comput. Simul. 76, 195–206. doi:10.1080/00949650412331321098

Willgoose, G., Bras, R.L., Rodriguez-Iturbe, I., 1991. A physical explanation of an observed link area-slope relationship. Water Resour. Res. 27, 1697–1702. doi:10.1029/91WR00937

Wolman, M.G., 1955. The Natural Channel of Brandywine Creek Pennsylvania, Geological Survey Professional Paper 271.

Wong, T.S.W., 2001. Formulas for time of travel in channel with upstream inflow. J. Hydrol. Eng. 6, 416–422.

Wong, T.S.W., 1995. Time of concentration formulae for planes with upstream inflow. Hydrol. Sci. J. 40, 663–666. doi:10.1080/02626669509491451

Xia, J., Wang, G., Tan, G., Ye, A., Huang, G.H., 2005. Development of distributed time-variant gain model for nonlinear hydrological systems. Sci. China Ser. D 48, 713–723. doi:10.1360/03yd0183

Zernitz, E.R., 1932. Drainage Patterns and Their Significance. J. Geol. 40, 498–521. doi:10.1086/623976

Zoch, R.T., 1934. On the relation between rainfall and stream flow. Mon. Weather Rev. 62, 315–322. doi:10.1175/1520-0493(1934)62<315:otrbra>2.0.co;2

Zuazo, V., Gironás, J., Niemann, J.D., 2014. Assessing the impact of travel time formulations on the performance of spatially distributed travel time methods applied to hillslopes. J. Hydrol. 519, 1315–1327. doi:10.1016/j.jhydrol.2014.09.035